


Posttranslational modification impact on the mechanism by which amyloid- β induces synaptic dysfunction

Katarzyna M Grochowska¹, PingAn Yuanxiang¹, Julia Bär^{1,2}, Rajeev Raman¹, Gemma Brugal^{3,4}, Giriraj Sahu¹, Michaela Schweizer⁵, Arthur Bikbaev⁶, Stephan Schilling⁷, Hans-Ulrich Demuth⁷ & Michael R Kreutz^{1,8,9,*} 

Abstract

Oligomeric amyloid- β (A β) 1-42 disrupts synaptic function at an early stage of Alzheimer's disease (AD). Multiple posttranslational modifications of A β have been identified, among which N-terminally truncated forms are the most abundant. It is not clear, however, whether modified species can induce synaptic dysfunction on their own and how altered biochemical properties can contribute to the synaptotoxic mechanisms. Here, we show that a prominent isoform, pyroglutamated A β 3(pE)-42, induces synaptic dysfunction to a similar extent like A β 1-42 but by clearly different mechanisms. In contrast to A β 1-42, A β 3(pE)-42 does not directly associate with synaptic membranes or the prion protein but is instead taken up by astrocytes and potently induces glial release of the proinflammatory cytokine TNF α . Moreover, A β 3(pE)-42-induced synaptic dysfunction is not related to NMDAR signalling and A β 3(pE)-42-induced impairment of synaptic plasticity cannot be rescued by D1-agonists. Collectively, the data point to a scenario where neuroinflammatory processes together with direct synaptotoxic effects are caused by posttranslational modification of soluble oligomeric A β and contribute synergistically to the onset of synaptic dysfunction in AD.

Keywords amyloid- β 1-42; amyloid- β 3(pE)-42; Jacob; N-methyl-D-aspartate-receptor; TNF α

Subject Categories Molecular Biology of Disease; Neuroscience; Post-translational Modifications, Proteolysis & Proteomics

DOI 10.15252/embr.201643519 | Received 13 October 2016 | Revised 13 March 2017 | Accepted 17 March 2017 | Published online 18 April 2017

EMBO Reports (2017) 18: 962–981

Introduction

Numerous studies indicate that soluble A β oligomers play a key role in the onset of synaptic dysfunction in early stage AD [1,2]. However, the molecular identity of the A β peptides that cause synapse loss and impair synaptic plasticity is still largely unclear. Multiple posttranslationally modified (PTM) A β peptides were found in brains of AD patients [3–5] and among these, N-terminally modified peptides are the most prominent species [3,6,7]. In particular, the amino-terminally truncated, pyroglutamated form of A β (A β 3(pE)-42) is abundant [8–10] and was shown to seed highly toxic co-oligomers with conventional A β 1-42 [11–13]. A β 3(pE)-42 exhibits distinct structural features that might carry specific neurotoxic activity [9,11,13–15].

Although a plethora of different A β 1-42 targets have been identified, relatively little is known about target interactions of PTM A β peptides and molecular mechanisms of their action. A pressing matter is whether PTM A β species can induce synaptic dysfunction on their own and if yes whether they induce neuronal pathology by different means. One influential view of the molecular mechanism that underlies synaptic dysfunction induced by full-length A β 1-42 focuses on N-methyl-D-aspartate-receptor (NMDAR) [16–19] and metabotropic glutamate receptor-5 (mGlu5) signalling [20–22]. This signalling is likely modulated through an association of A β oligomers to the prion protein (PrP) [23–25]. Binding of A β 1-42 to the extracellular domain of the PrP results in abnormal activation of Fyn tyrosine kinase, a signalling event that has been shown to play an important role in A β -induced synaptic pathology [23–25]. A β 1-42-PrP-dependent Fyn activation is mediated by mGlu5-activation [26], and A β 1-42-induced synaptic dysfunction most likely depends

1 RG Neuroplasticity, Leibniz Institute for Neurobiology, Magdeburg, Germany

2 Emmy-Noether Group "Neuronal Protein Transport", Center for Molecular Neurobiology ZMNH, University Medical Center Hamburg-Eppendorf, Hamburg, Germany

3 Department of Biochemistry and Molecular Biology, Faculty of Biology, Centro de Investigación Biomédica en Red Sobre Enfermedades Neurodegenerativas, University of Barcelona, Barcelona, Spain

4 Institute of Biomedicine of the University of Barcelona (IBUB), Barcelona, Spain

5 Morphology Unit, Center for Molecular Neurobiology ZMNH, University Medical Center Hamburg-Eppendorf, Hamburg, Germany

6 RG Molecular Physiology, Leibniz Institute for Neurobiology, Magdeburg, Germany

7 Department of Drug Design and Target Validation MWT, Fraunhofer Institute of Cell Therapy and Immunology IZI Leipzig, Halle, Germany

8 Leibniz Group "Dendritic Organelles and Synaptic Function", Center for Molecular Neurobiology ZMNH, University Medical Center Hamburg-Eppendorf, Hamburg, Germany

9 German Center for Neurodegenerative Diseases, Magdeburg, Germany

*Corresponding author. Tel: +49 391 626394181; E-mail: kreutz@lin-magdeburg.de

upon a functional and possibly also physical interaction of NMDAR, PrP and mGlu5.

In addition, inflammatory processes are thought to further aggravate synaptic loss already at the early stages of sporadic AD. Numerous cytokines such as TNF α , IL-1 β or IL-6 were reported to be upregulated in AD brain and could potentially aggravate disease progression [27–29]. In particular, TNF α was shown to influence A β production, increase oligomer-induced apoptosis and mediate A β -induced long-term potentiation (LTP) [28]. To address the question whether PTM A β species might contribute to early synaptic dysfunction by divergent mechanisms, we utilised the conceptual framework outlined above.

Results

Characterisation of A β oligomers

A β monomers, oligomers and fibrils have different effects on neuronal function, and mainly higher-order oligomers are synaptotoxic and induce early synaptic dysfunction in AD [1–3]. A β 1-42 and A β 3(pE)-42 oligomer production was monitored and controlled by different means. SDS-PAGE (Fig EV1A) followed by immunodetection with antibodies detecting the N-terminus of A β oligomers (82E1 for A β 1-42 and Abeta-pE3 for A β 3(pE)-42) indicated that both preparations resulted in a spectrum of oligomeric A β species, from low (2–4mers) to high-n oligomers (12–48mers) in accordance with other studies [2], a result that was confirmed by size-exclusion chromatography and subsequent ELISA quantification (Fig EV1E). A similar pattern with a slight shift towards higher molecular weight forms was observed for A β 3(pE)-42 (Fig EV1A). Transmission electron microscopy (TEM) of both preparations revealed globular, oligomeric structures of various sizes. In both preparations, no fibrillar or protofibrillar species were observed (Fig EV1B). The preparation was further characterised by dynamic light scattering (DLS), showing that both A β 1-42 and A β 3(pE)-42 oligomers form a broad range of species, distinct from monomers and fibrils (Fig EV1C). Furthermore, 8-anilino-1-naphthalene-sulfonic acid (ANS) fluorescence spectroscopy revealed

conformational differences between oligomeric, monomeric and fibrillar preparations for both species (Fig EV1D). A β preparations were also separated by native PAGE which revealed a similar distribution pattern of both species (Fig EV1F). Thus, both preparations yielded comparable larger oligomers that are considered to be most synaptotoxic in the onset of AD. We also used A β 1-42 and A β 3(pE)-42 fibril preparations as a control in some experiments outlined below as well as a control for DLS and ANS studies (Fig EV1C and D). Fibril production was additionally monitored by a Thioflavin T (ThT) assay (Fig EV2A).

A β 1-42 and A β 3(pE)-42 oligomers induce both synapse loss and dysfunction

Synapse loss in the hippocampus is an early neuropathological hallmark in AD that strongly correlates with cognitive impairment. In the first set of experiments, we wanted to address whether application of both, oligomeric A β 1-42 and A β 3(pE)-42, to hippocampal primary neurons impacts in a comparable manner on synapse number. We indeed found that treatment of either A β oligomer species at a concentration of 500 nM applied to DIV17 neurons for 3 days resulted in a reduced number of synapses (Fig 1A and B). Fibrils of both A β species had no effect on synapse number as compared to non-treated cultures (Fig EV2D and E). Interestingly, both A β oligomers also induced a clear reduction in dendrite complexity as evidenced by Sholl analysis (Fig 1C and D), and in this case, the effect of A β 3(pE)-42 was more pronounced than those of A β 1-42 (Fig 1C and D).

Additionally, acute application of A β 3(pE)-42 like A β 1-42 significantly reduced the mEPSC frequency and amplitude of hippocampal primary neurons patched in the whole-cell mode (Fig 1E–G), indicating that both oligomeric A β species induce acute synaptic dysfunction and depression to a comparable extent. Similar results were obtained when we looked at spontaneous Ca²⁺ spikes with Ca²⁺ imaging in hippocampal primary neurons after bath application of both oligomers for 3 days. A β 1-42 and A β 3(pE)-42 both reduced the number of synchronous Ca²⁺ spikes as evidenced by Fluo-4 AM Ca²⁺ imaging (Fig 1H and I). Thus, both oligomers also suppress neuronal network activity (Fig 1H and I).

Figure 1. Effects of A β oligomers on synapse density, dendritic tree complexity, mEPSC amplitude and frequency, and neuronal network activity.

- A Both A β 1-42 and A β 3(pE)-42 cause synaptic loss. Representative confocal images of dendrites used for quantification. Scale bar, 5 μ m.
- B Bar plot representing synaptic density of DIV20 neurons stained for Homer1, Synaptophysin and MAP2 after treatment with 500 nM A β 1-42 or A β 3(pE)-42 for 3 days compared to non-treated controls. *n* corresponds to the number of separate dendritic segments on different neurons analysed from at least three independent coverslips and at least two independent cell cultures.
- C Both A β 1-42 and A β 3(pE)-42 cause simplification of the dendritic tree. The graph represents the results of a Sholl analysis of GFP-transfected neurons treated with A β 1-42 (*n* = 23) or A β 3(pE)-42 (*n* = 25) and corresponding controls (*n* = 25). *n* corresponds to the number of neurons analysed from at least three independent coverslips and at least three independent cell cultures.
- D Images of representative neurons. Scale bar, 100 μ m.
- E A β 1-42 and A β 3(pE)-42 cause a decrease in mEPSC amplitude and frequency. Example traces of mEPSCs in neurons treated with A β 1-42 and A β 3(pE)-42.
- F, G Cumulative probability plot and bar graph illustrating effects of A β 1-42 and A β 3(pE)-42 treatment on mean amplitude (F) or frequency of mEPSCs (G). *n* corresponds to the number of neurons analysed from at least four independent cell cultures.
- H Example traces from Ca²⁺ imaging. Four to six cells from the same scan are depicted with different colours.
- I Treatment for 3 days with A β 1-42 or A β 3(pE)-42 caused a decrease in the frequency of synchronised calcium waves. Co-application of ifenprodil rescues the phenotype caused by A β 1-42 but not those of A β 3(pE)-42 application. *n* corresponds to the number of independent coverslips from at least four independent cell cultures.

Data information: *P*-values, unless indicated otherwise in the graph, refer to control by one-way ANOVA. Data are represented as the mean \pm s.e.m. For a Sholl analysis, two-way ANOVA followed by an unpaired two-tailed Student's *t*-test was used. *P*-values in red refer to A β 3(pE)-42 compared to control, in grey A β 1-42 compared to control and in black between oligomers within the same distance from soma.

Oligomeric A β 1-42 and A β 3(pE)-42 induce CREB shut-off and nuclear accumulation of Jacob

The subcellular localisation of NMDAR profoundly and differentially affects the nuclear response following activation. Stimulation of synaptic NMDAR induces the expression of cell survival and plasticity genes, while their extrasynaptic counterparts primarily drive the expression of cell death genes, linking the latter pathway to disease

[30,31]. One hallmark of extrasynaptic NMDAR signalling in AD is a de-phosphorylation and transcriptional inactivation of the transcription factor cAMP response element binding protein (CREB) [32]. Jacob is a protein that encodes the synaptic and extrasynaptic origin of NMDAR signals to the nucleus [33], and in previous work, we found that Jacob links extrasynaptic A β 1-42-GluN2B signalling to altered CREB-dependent gene expression [34,35]. Nuclear import of Jacob following extrasynaptic NMDAR stimulation results in

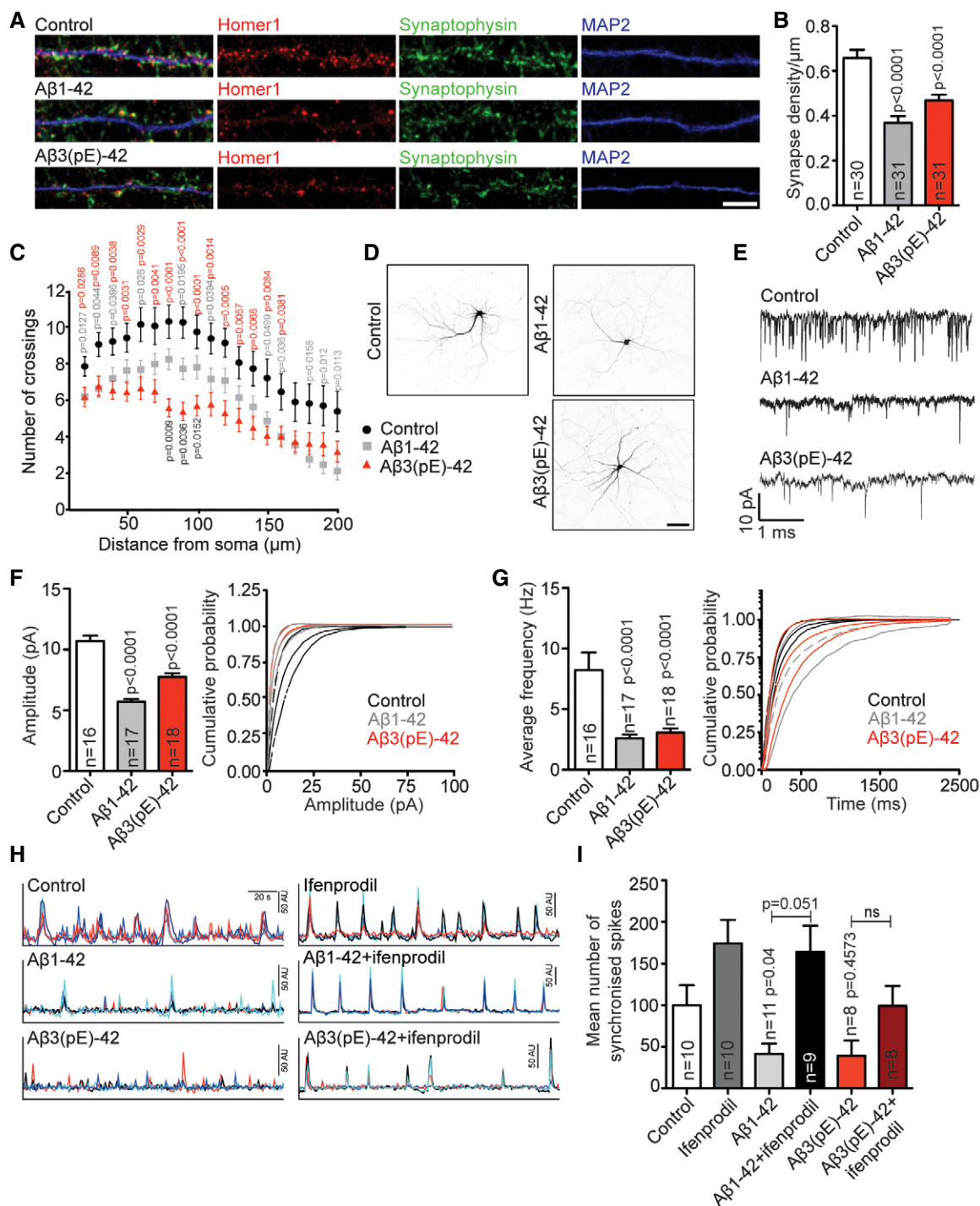


Figure 1.

sustained de-phosphorylation of CREB, a stripping of synaptic contacts, simplification of the dendritic tree and finally cell death [33,36]. In case of A β 1-42, CREB shut-off depends on the sustained

activation of extrasynaptic GluN2B-containing NMDAR [35,37,38] and the subsequent nuclear import of Jacob [34,35]. We next asked whether also A β 3(pE)-42 is capable of inducing CREB shut-off and

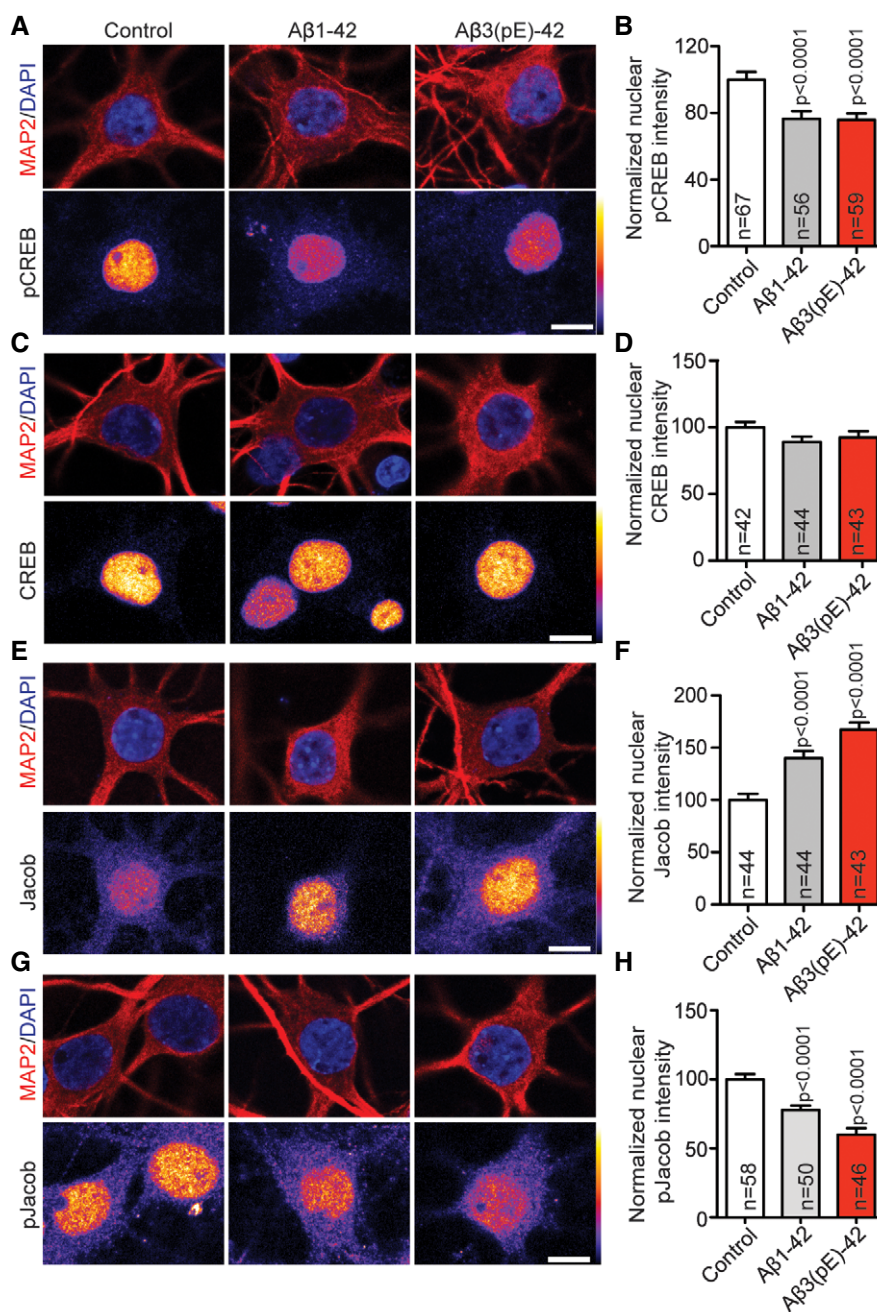


Figure 2. A β 1-42 and A β 3(pE)-42 induce CREB shut-off, drive Jacob in the nucleus and decrease nuclear pJacob levels.

Confocal images averaged from two sections of the nucleus of DIV18 primary hippocampal neurons stained for MAP2 and DAPI.

A, B (A) Neurons were co-stained for pCREB (Ser133) and (B) the quantification revealed the decrease in nuclear pCREB immunoreactivity after treatment with A β 1-42 and A β 3(pE)-42.

C, D No change of total CREB levels was observed in nucleus of neurons co-stained for pan-CREB.

E–H There is an increase in nuclear Jacob immunoreactivity of neurons co-stained with a pan-Jacob antibody upon A β oligomers treatment (E, F) as well as a decrease in nuclear pJacob immunoreactivity (G, H). For the quantified channel (pCREB, CREB, pan-Jacob and pJacob), original pixel intensities from 0 to 255 are represented as a gradient lookup table.

Data information: Scale bars, 10 μ m. *n* corresponds to the number of nuclei from different neurons analysed from at least four independent coverslips and at least three independent cell cultures. *P*-values versus control, by one-way ANOVA. Data are represented as mean \pm s.e.m.

indeed found significantly reduced pCREB immunofluorescence (Fig 2A and B), whereas nuclear CREB immunofluorescence was not altered (Fig 2C and D). Interestingly, oligomeric A β 3(pE)-42 also induced nuclear accumulation of Jacob like it was shown previously for A β 1-42 [35] (Fig 2E and F). Moreover, treatment with both A β peptides resulted in significantly reduced pJacob immunostaining intensity in the nucleus (Fig 2G and H), indicating nuclear import of non-phosphorylated Jacob, capable of inducing CREB shut-off following activation of GluN2B-containing extrasynaptic NMDAR [33]. Application of fibrils of both A β isoforms had no effect on CREB phosphorylation, indicating that only oligomeric A β 1-42 and A β 3(pE)-42 trigger pathological signalling to the nucleus (Fig EV2B and C).

The D1-agonist SKF38393 rescues A β 1-42 but not A β 3(pE)-42-induced impairment of LTP

Collectively, the data so far show that both A β oligomers have comparable effects on synapse loss, synaptic dysfunction, network activity and signalling to the nucleus. One well-documented consequence of A β 1-42-induced synaptic dysfunction that supposedly contributes to cognitive dysfunction in AD is an impairment of LTP at hippocampal CA1 synapses [35,37,39–41]. We therefore next evaluated whether both peptides might also limit synaptic plasticity in this cellular model of learning and memory. Bath perfusion of A β 3(pE)-42 like A β 1-42 2 h prior to high frequency stimulation caused a significantly reduced LTP after tetanisation (Fig 3A–C and I). Both oligomers had no effect on baseline recordings of fEPSP (Fig 3D), did not prevent induction of early LTP and reduced the magnitude of late LTP to a similar degree (Fig 3B, C and I). In previous studies, it was shown that administration of dopamine D1/D5 receptor agonists prevents the LTP impairment induced by conventional A β 1-42 [39,41]. In accord with these results, co-perfusion of the D1/D5 agonist SKF38393 during tetanisation prevented the A β 1-42-induced decline in late LTP (Fig 3F, G and I). In contrast and much to our surprise, the D1R/D5R agonist failed to rescue LTP in slices treated with A β 3(pE)-42 under identical conditions (Fig 3H and I). This result indicates that A β 1-42 and A β 3(pE)-42 might activate distinct synaptic signalling pathways that interfere with the expression of LTP at hippocampal CA1 synapses.

A β 3(pE)-42 does not bind to the PrP and pre-blocking with anti-PrP antibody does not prevent A β 3(pE)-42-induced CREB shut-off

We therefore asked next about the signalling pathways that might be activated differentially by both A β species. The PrP protein plays a documented role for synaptic dysfunction induced by full-length oligomeric A β 1-42 [23–25] and is considered to be an important high-affinity A β receptor at synaptic membranes [23,24,26,42]. Previous work has shown that binding of A β 1-42 drives an interaction of the PrP with mGlu5 to emanate a signal that causes activation of Fyn, an essential player in a cascade of events that ultimately leads to NMDAR-mediated excitotoxicity and hyper-phosphorylation of tau [23]. Surprisingly, we found that in contrast to A β 1-42, A β 3(pE)-42 did not associate with PrP heterologously expressed at the cell surface of HEK293T cells (Fig 4A). We therefore wondered whether association with the PrP is also instrumental for long-distance signalling of A β 1-42 to the nucleus. Support for this notion came from experiments where we could block A β 1-42-induced

CREB shut-off with a PrP blocking antibody that masks the A β 1-42 binding site in the protein (Fig 4B and C). No CREB shut-off was visible after co-application of A β 1-42 oligomers and 30 min pre-blocking with the PrP antibody in hippocampal primary neurons (Fig 4B and C). In contrast, bath application of this antibody could not prevent A β 3(pE)-42-induced CREB shut-off (Fig 4B and C).

It was also reported that A β 1-42 clusters mGlu5 [20] and might displace NMDAR from synaptic sites, in a manner that might involve a *cis*-interaction between the GluN1 subunit of NMDAR and mGlu5 [43]. We therefore investigated whether binding of A β 1-42 to the PrP might affect this interaction and whether all three proteins might interact in *cis*. To address this question, we performed a bioluminescence resonance energy transfer (BRET) assay (Fig 4D) in HEK293T cells and we indeed found that application of A β 1-42 triggered an increase in BRET efficiency, indicating a stronger interaction between NMDAR and mGlu5 only in presence of PrP (Fig 4D–F). This increase was not evident after administration of A β 3(pE)-42 (Fig 4H and I), suggesting that the PrP is not a high-affinity receptor for A β 3(pE)-42 and will not induce synaptic dysfunction via aberrant PrP-mGlu5-NMDAR signalling.

A β 3(pE)-42-induced CREB shut-off, impaired network oscillation and synapse loss cannot be rescued by the GluN2B antagonist ifenprodil

Collectively, these data suggest that both A β peptides have different primary targets and will induce synaptic dysfunction by different mechanisms. To learn more about these mechanisms, we next focussed on extrasynaptic GluN2B-containing NMDAR. Previous studies have shown that bath application of oligomeric A β 1-42 decreases spontaneous neuronal network activity and induces retraction of synaptic contacts and dendrites and CREB shut-off in a manner that requires signalling of extrasynaptic GluN2B-containing NMDAR [35]. We therefore asked first whether the detrimental immediate effects of oligomeric A β 3(pE)-42 administration can be prevented by bath application of a GluN2B antagonist. In contrast to A β 1-42, inclusion of the GluN2B antagonist ifenprodil did not completely block the effect of A β 3(pE)-42 application on neuronal network activity as evidenced by Fluo-4 AM Ca²⁺ imaging (Fig 1H and I). As reported previously [35], A β 1-42-induced CREB shut-off can be blocked with the GluN2B-NMDAR antagonist ifenprodil confirming that activation of downstream effectors of these receptors is involved in early detrimental actions of this oligomer (Appendix Fig S1A and B). However, co-application of ifenprodil could not prevent de-phosphorylation of CREB following inclusion of oligomeric A β 3(pE)-42 in the medium (Appendix Fig S1A and B). Similarly, A β 1-42- but not A β 3(pE)-42-induced loss of synaptic contacts could be blocked by ifenprodil (Appendix Fig S1C and D), indirectly suggesting that also the structural damage caused by oligomeric A β 3(pE)-42 is not mediated by activation of GluN2B-containing NMDAR. Thus, A β 3(pE)-42 oligomers induce early neuronal dysfunction neither by activation of GluN2B-containing NMDARs nor the PrP.

A β 3(pE)-42 does not associate with neuronal membranes and is efficiently taken up by astrocytes

The primary cultures that we used in all previous experiments contain neurons and astrocytes. In the light of the findings

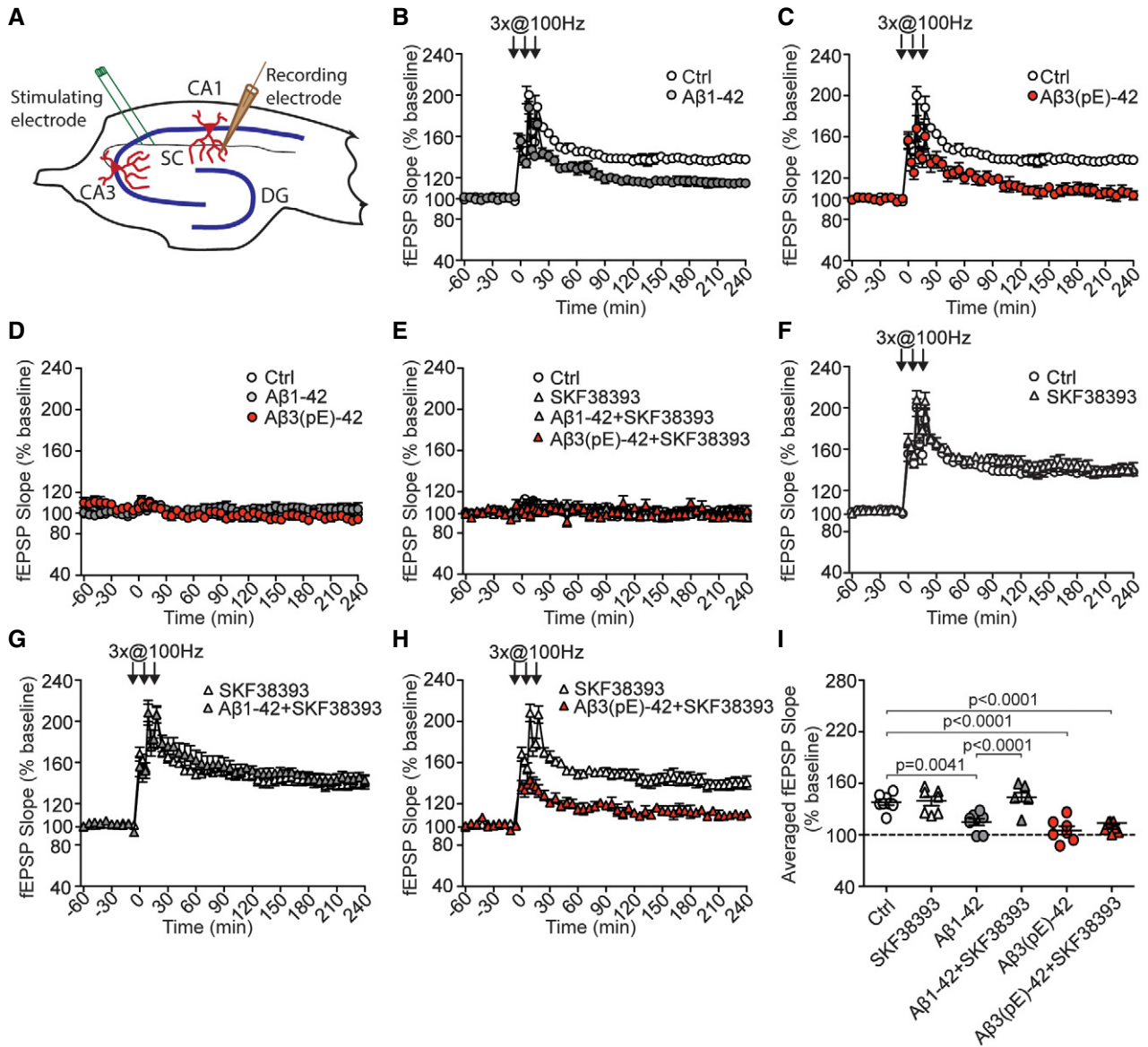


Figure 3. An agonist of dopamine D1/D5 receptors selectively rescues late LTP impaired by Aβ1-42, but not Aβ3(pE)-42.
A–C (A) Schematic representation of electrode positioning in acute hippocampal slice. LTP recordings revealed that both (B) Aβ1-42 ($n = 8$) and (C) Aβ3(pE)-42 ($n = 7$) cause impairment of late phase LTP compared to control measurements ($n = 8$).
D Basal synaptic transmission is not affected by bath application of Aβ1-42 ($n = 8$) or Aβ3(pE)-42 ($n = 7$) oligomers.
E Basal synaptic transmission is not affected by dopamine D1/D5 receptor agonist SKF38393 ($n = 7$) applied alone or together with Aβ oligomers ($n = 7$ in each group).
F Application of SKF38393 in control conditions does not alter tetanisation-triggered LTP.
G, H Activation of D1/D5 receptors by SKF38393 restores the CA1 LTP in Aβ1-42-treated ($n = 7$), but not Aβ3(pE)-42-treated slices ($n = 7$).
I Dot plot representing averaged fEPSP slope. P -values versus control by one-way ANOVA.
Data information: All data come from the same experiments where a group of slices were treated with oligomers with or without SKF38393. n corresponds to the number of slices from at least three mice. Data are represented as mean \pm s.e.m.

above, we next examined with antibody staining how both oligomers are localised after bath application for 40 min in hippocampal primary cultures. Immunostaining with antibodies directed against the N-terminus of Aβ oligomers (82E1 for Aβ1-42 and Abeta-pE3 for Aβ3(pE)-42) revealed that oligomeric Aβ1-42 expectedly associates prominently with neuronal membranes

(Fig 5A). This was in contrast to the diffuse staining of oligomeric Aβ3(pE)-42 (Fig 5B). On the contrary, Aβ1-42 does not associate prominently with astroglia (Fig 5C), while the majority of Aβ3(pE)-42 was present in somatic inclusions within astrocytes, as revealed by three-dimensional reconstruction of confocal images (Fig 5D). This was further confirmed in

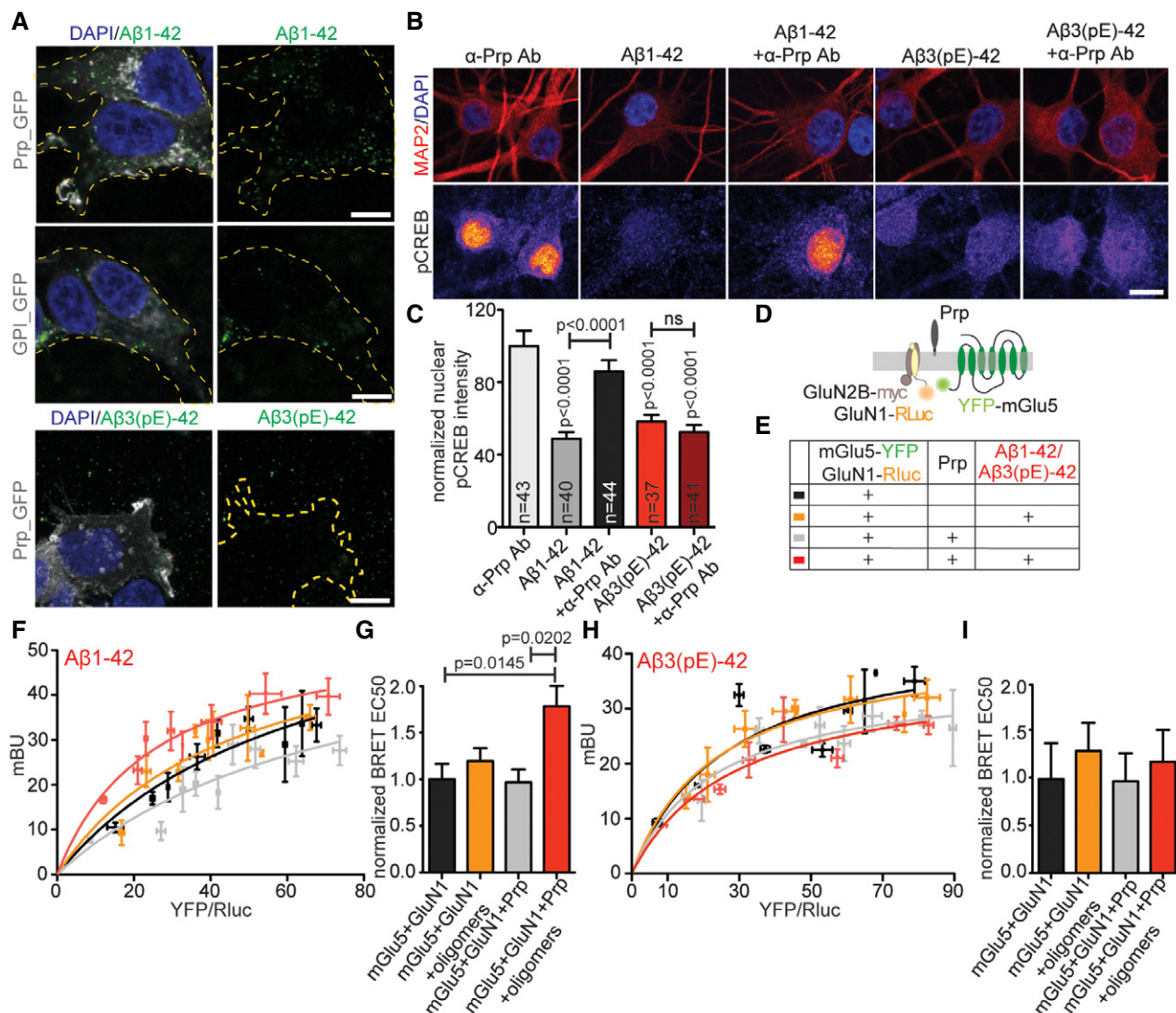


Figure 4. A β 3(pE)-42 neurotoxic effects do not involve PrP-dependent signalling pathways.

A Confocal images of HEK293T cells overexpressing GPI-GFP or PrP-GFP treated with A β 1-42 or A β 3(pE)-42. Only A β 1-42 specifically associates with cells overexpressing PrP. Scale bar, 10 μ m.

B Images averaged from two confocal sections of the nucleus of primary hippocampal neurons (DIV18) stained for pCREB and MAP2. Original pixel intensities from 0 to 255 are represented as a gradient lookup table. Scale bar, 10 μ m.

C Pre-treatment with antibody (Ab) blocking PrP-A β binding site rescued A β 1-42-, but not A β 3(pE)-42-, mediated CREB shut-off. *n* corresponds to the number of nuclei from different neurons analysed from at least four independent coverslips and at least two independent cell cultures.

D Scheme representing BRET experiments performed to assess the influence of PrP and A β oligomers on mGlu5 and GluN1.

E Colour code and explanation of transfection and treatment combinations for experimental groups analysed in (F–I).

F BRET curves showing amount of energy transfer (mBU) depending on growing donor/acceptor ratio for cells treated with A β 1-42.

G Bar plots representing mean BRET EC₅₀ values. Only in presence of PrP-A β 1-42 causes significant increase in energy transfer kinetics.

H BRET curves showing the amount of energy transfer (mBU) depending on growing donor/acceptor ratio for cells treated with A β 3(pE)-42.

I Bar plots representing mean BRET EC₅₀ values. A β 3(pE)-42 does not enhance the kinetics of mGlu5-GluN1 interaction.

Data information: *P*-values versus control by one-way ANOVA. Data are represented as mean \pm s.e.m. In (F–I) BRET data are represented as means \pm s.e.m. of 4–6 different experiments on independent HEK293T cells culture.

experiments where we transfected astrocytes with myristoylated GFP as a cell membrane marker (Fig 5E). Next, we asked whether co-oligomers of A β 1-42 and A β 3(pE)-42 will also associate with glia. The immunostainings followed by three-dimensional reconstruction revealed that some co-oligomers form also somatic inclusions in astrocytes (Fig 5F).

A β 3(pE)-42 does not induce synapse loss, nuclear translocation of Jacob and CREB shut-off in hippocampal cultures with low glia content

The preparation protocol for hippocampal primary cultures includes several steps that are not in favour of microglia attachment.

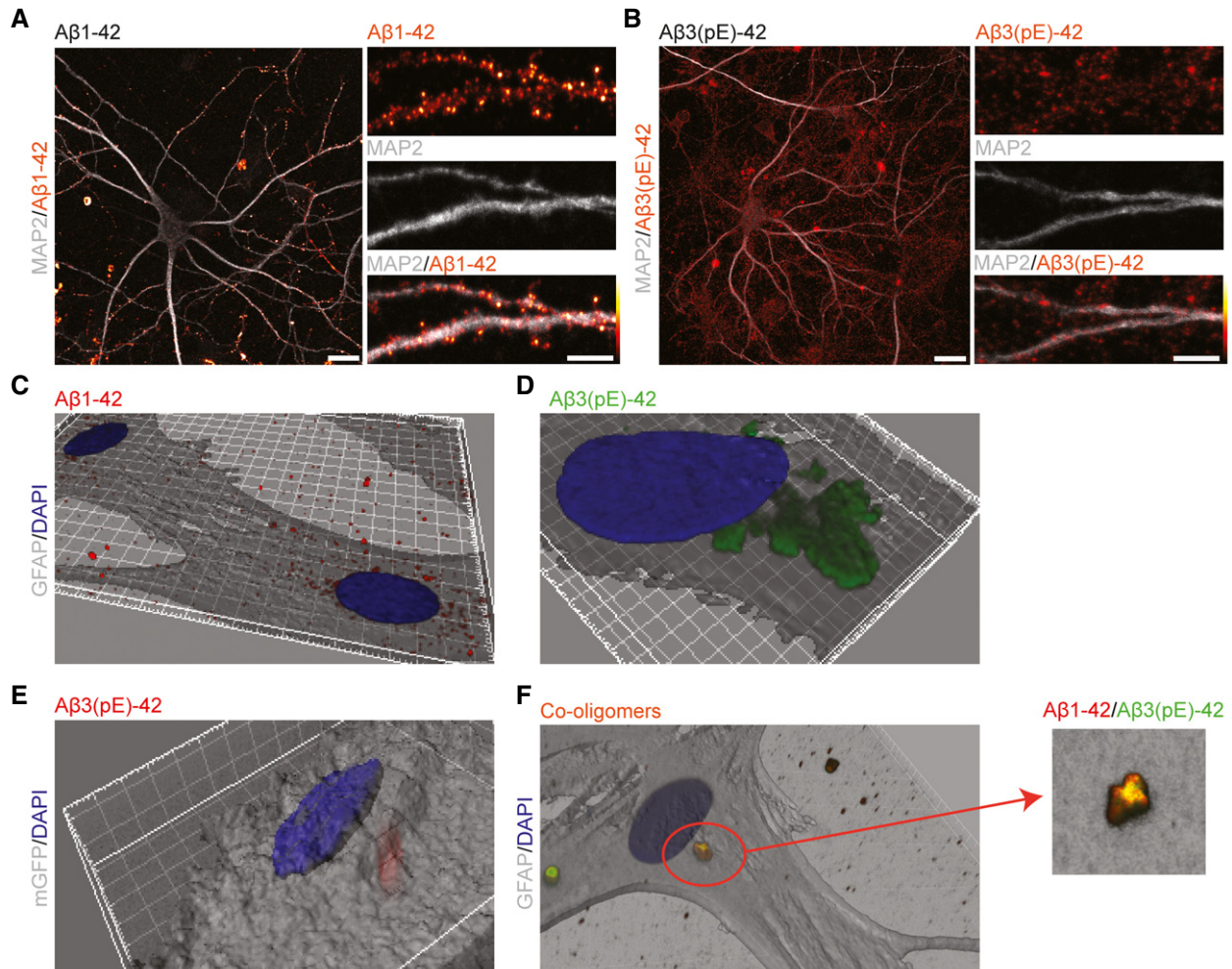


Figure 5. A β 3(pE)-42 does not bind prominently to neuronal membranes but is instead taken up efficiently by astrocytes.

- A, B Confocal images of DIV18 neurons stained for (A) A β 1-42 or (B) A β 3(pE)-42 after 40 min of treatment demonstrate that A β 1-42 associates preferentially with neuronal membranes, whereas A β 3(pE)-42 is rather diffusely distributed in mixed neuronal culture. Scale bars, 10 μ m (images of a whole neuron) and 5 μ m (zoomed in panels).
- C, D 3D reconstructions (based on GFAP) of confocal images of astrocytes indicate that A β 3(pE)-42, but not A β 1-42, is taken up by astrocytes after 40 min of treatment.
- E 3D reconstruction of an astrocyte transfected with mGFP revealed that A β 3(pE)-42 localises within the cell 40 min following application.
- F Co-oligomerisation of A β 1-42 and A β 3(pE)-42 causes association of both species in one structure and leads to astrocytic uptake not only of A β 3(pE)-42 but also A β 1-42.

We indeed found no evidence for the presence of microglia in these cultures before and after treatment with oligomers by means of immunocytochemistry (ICC) or immunoblotting using Iba-1 as a marker (Appendix Fig S2C and D). The tight association of A β 3(pE)-42 with glial cells led us then to reason that astroglia might also contribute to A β 3(pE)-42-induced pathology. To test this notion, we treated hippocampal primary cultures on DIV5 with 200 nM cytosine arabinoside (AraC) to suppress mitosis and glia proliferation (Appendix Fig S2A and B). This treatment resulted in an approximately 11-fold reduction in astrocyte content in these mixed cultures (Appendix Fig S2A and B). Remarkably, oligomeric A β 3(pE)-42-induced synapse loss was absent in cultures with a low astroglia content (Fig 6A–C). Following AraC treatment, we also observed no longer a significant effect of A β 3(pE)-42 administration on CREB phosphorylation, nuclear accumulation of Jacob or on the decrease

in nuclear pJacob immunofluorescence (Fig 6D–K). On the contrary, A β 1-42 treatment induced nuclear translocation of non-phosphorylated Jacob, CREB shut-off and a reduction in synapse number irrespective of the astroglia content of the primary cultures (Fig 6B–K).

A β 3(pE)-42 causes stronger microglia activation and astroglia proliferation in organotypic hippocampal slices than A β 1-42

Reactive astrocytes are an integral part of the neuroinflammatory response in AD. We corroborated these findings in organotypic hippocampal slice cultures treated with either of the two oligomeric A β isoforms. Immunohistochemical staining for reactive microglia with an antibody directed against Iba-1, a marker of activated microglia, revealed that A β 3(pE)-42 caused a much more prominent microglia activation than administration of A β 1-42 (Fig EV3A and

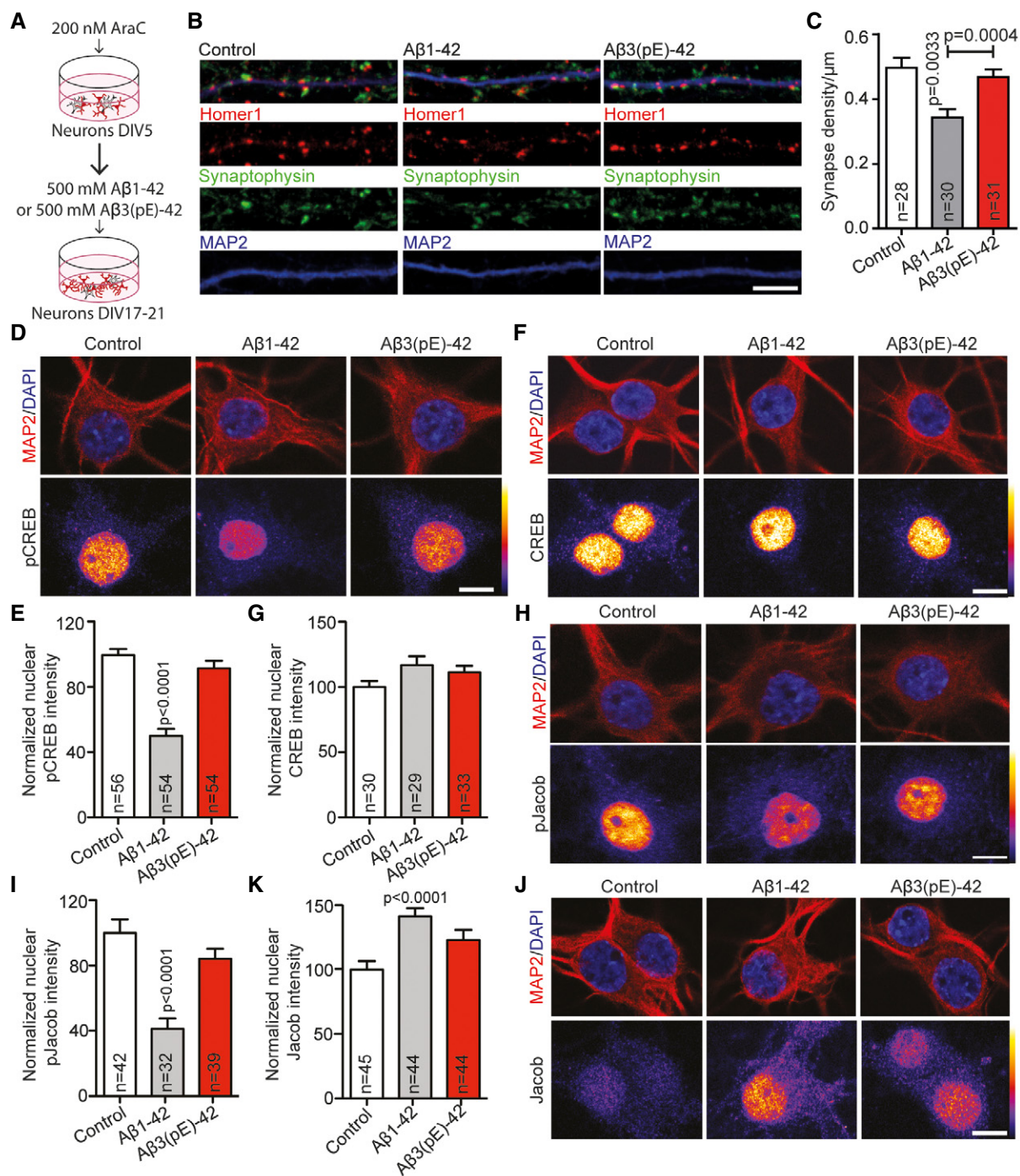


Figure 6. In AraC-treated cultures A β 3(pE)-42 does not cause synapse loss, de-phosphorylation of pCREB and accumulation of non-phosphorylated Jacob in the nucleus.

A Scheme representing the AraC treatment regime of neuronal cultures at DIV5.
B Confocal images of representative dendrites, stained for Homer1, Synaptophysin and MAP2, demonstrating that the decrease in synaptic density in AraC-treated cultures was evident only after A β 1-42 application. Scale bar, 5 μ m.
C Treatment with AraC selectively prevents the decrease in the mean synaptic density after A β 3(pE)-42 application. *n* corresponds to the number of separate dendritic segments on different neurons analysed from at least three independent coverslips and at least two independent cell cultures.
D–K (D, E) In AraC-treated cultures, only A β 1-42, but not A β 3(pE)-42, causes decrease in pCREB nuclear staining intensity with (F, G) unchanged CREB levels. Also (H, I) the pJacob nuclear levels and (J, K) Jacob accumulation significantly changes only in case of A β 1-42 treatment. Original pixel intensities from 0 to 255 are represented as a gradient lookup table. Scale bar, 10 μ m.

Data information: *n* corresponds to the number of nuclei from different neurons analysed from at least four independent coverslips and at least three independent cell cultures. *P*-values versus control, by one-way ANOVA. Data are represented as mean \pm s.e.m.

B). We next quantified astroglia proliferation with GFAP immunohistochemistry in slices following addition of A β oligomers to the medium, and we found that the presence of A β 3(pE)-42 resulted in increased GFAP staining intensity, while A β 1-42 applied at the same concentration had only a minor effect (Fig EV3C and D). Taken together, these results suggest that microglia activation and astroglial proliferation in AD is prominently triggered by A β 3(pE)-42 and might be linked to early neuronal dysfunction.

The astrocytic release of TNF α is increased in response to A β 3(pE)-42 and less to A β 1-42

Microglia is rare in hippocampal primary cultures and staining with an Iba-1 antibody or SDS-PAGE of cell culture extract yielded negative results (Appendix Fig S2C and D). To gain further mechanistic insights, we therefore investigated astrocytic release of potential synaptotoxic factors. We focussed on TNF α because this cytokine is released from micro- and astroglia in the primary stage of neuroinflammation in AD and has a documented role in synaptic downscaling and alterations [44–47]. A TNF α ELISA to quantify this proinflammatory cytokine revealed elevated TNF α levels in the astrocyte lysate treated for 13 h with A β 3(pE)-42, whereas A β 1-42 induced a much smaller increase (Fig 7A).

Conditioned medium from astrocytes treated with A β 3(pE)-42 causes synapse loss and CREB shut-off

We next directly tested the hypothesis that glial release of TNF α following stimulation of A β 3(pE)-42 is crucial for subsequent synapse loss and CREB shut-off. To this end, we treated primary astrocyte cultures with A β 3(pE)-42 or conventional A β 1-42 oligomers for 40 min. Conditioned media was then collected, and hippocampal neurons were supplemented with this medium for 40 min (Fig 7B). The A β concentration in the media was below the detection limit (< 12.5 pg/ml) of an ELISA that is suitable for quantification of both peptide species. Treatment of primary hippocampal cultures with conditioned medium induced statistically significant synapse loss only in case of A β 3(pE)-42. Most important, synapse loss induced by A β 3(pE)-42 conditioned medium was rescued by application of a TNF α neutralising antibody (Fig 7C and D). Moreover, neurons treated with media from astrocyte cultures that were stimulated with A β 3(pE)-42 showed a significant decrease in nuclear pCREB immunofluorescence (Fig 7E and F). Conditioned medium from astrocyte cultures treated with similar concentrations of A β 1-42 had no effect (Fig 7E and F).

We next sought to determine whether the neutralising antibody is effective in mixed neuronal/glia cultures. Synapse loss caused by both A β oligomers could be fully rescued by co-application of the TNF α neutralising antibody only in case of A β 3(pE)-42-treated neurons (Fig 8A and B). Accordingly, the neutralising anti-TNF α antibody did not prevent CREB shut-off induced by A β 1-42 (Fig 8C and D), while it completely blocked A β 3(pE)-42-induced CREB shut-off (Fig 8C and D) without changing total CREB levels (Appendix Fig S3A and B). In addition, a TNFR1 peptide antagonist that blocks the interaction site of TNF α in TNFR1 [48,49] also prevented A β 3(pE)-42- but not A β 1-42-induced CREB shut-off (Fig EV4A and B). Finally, we could rescue the detrimental effect of oligomeric A β 3(pE)-42 on the maintenance of LTP in CA1 of acute

mouse hippocampal slices when we co-applied the neutralising anti-TNF α antibody (Fig 9A–F). The same treatment had very little effect on the A β 1-42-induced impairment of LTP (Fig 9A–F).

Collectively, these data point to a prominent role of TNF α in neuronal dysfunction induced by oligomeric A β 3(pE)-42. To directly test whether TNF α on its own can in principle induce structural damage in primary neurons, we bath-applied the cytokine and quantified synapse number and dendrite complexity (Fig EV5A–C). It turned out that application of TNF α indeed induced synapse loss and simplification of dendrites (Fig EV5A–C).

We then assessed whether intervention with TNF α signalling has a protective effect against synaptic dysfunction in mouse models of AD. To this end, we chose 5XFAD mice that express mutant APP and PSEN1 and accumulate high levels of A β 1-42. LTP is normal in young animals, but becomes impaired around 6 months [50]. Expectedly the fEPSP slope as a readout of LTP strength was therefore lower in acute hippocampal slices of 8-month-old 5XFAD mice than in corresponding control slices (Figs 10D–F and 3B, C and I). Application of the neutralising anti-TNF α antibody had no effect on the fEPSP slope (Fig 10E and F). In the TBA2.1 mouse model, A β 3(pE)-42 (expressed under control of a Thy-1 promoter) rapidly accumulates in the hippocampus, which results in synaptic dysfunction and memory impairment already in mice at the age 8–10 weeks [51]. Accordingly, the fEPSP slope and maintenance of late LTP are severely affected in these mice (Fig 10A–C). Most important, in contrast to 5XFAD mice, inclusion of the neutralising anti-TNF α antibody almost restored late LTP and increased the fEPSP slope amplitude (Fig 10B and C). Collectively, these data point to a prominent role of TNF α in neuronal dysfunction induced by oligomeric A β 3(pE)-42 as compared to A β 1-42. Interestingly, the D1-agonist SKF38393 could not rescue LTP impairment in TBA2.1 which corroborates the finding that SKF38393 rescues A β 1-42- but not A β 3(pE)-42-induced LTP impairment (Fig 3G–I).

A β 3(pE)-42 and A β 1-42 induce neuronal dysfunction via a p38MAPK kinase pathway

We finally asked how pathological A β 3(pE)-42 and A β 1-42 signalling might converge to induce synapse loss and CREB shut-off. Published work demonstrates that TNF α and conventional A β 1-42 can both activate p38MAPK and that enhanced p38MAPK signalling is involved in synaptic dysfunction and impaired plasticity in caused by A β oligomers [52,53]. We therefore hypothesised that p38MAPK signalling might be a point of convergence for both A β pathways. To test this idea, we treated hippocampal primary neurons with A β 3(pE)-42 or A β 1-42 and co-applied the p38MAPK inhibitor SB203580 or a vehicle control. We then determined synapse loss, dendrite retraction and CREB shut-off. It turned out that treatment with both oligomers is sensitive to SB203580 application and that inhibition of p38MAPK attenuated synapse loss (Appendix Fig S4A and B) CREB shut-off (Appendix Fig S4C and D) as well as dendrite retraction (Appendix Fig S4E). Moreover, the p38MAPK inhibitor also attenuated TNF α -induced synapse loss and dendrite retraction (Fig EV5A–C). Finally, bath application of both oligomers resulted in enhanced phosphorylation and activation of p38MAPK (Appendix Fig S4F and G), while this treatment had no effect on p38MAPK protein levels (Appendix Fig S4H and I). Thus, activation of p38MAPK is a nodal point for pathological signalling evoked by both oligomers.

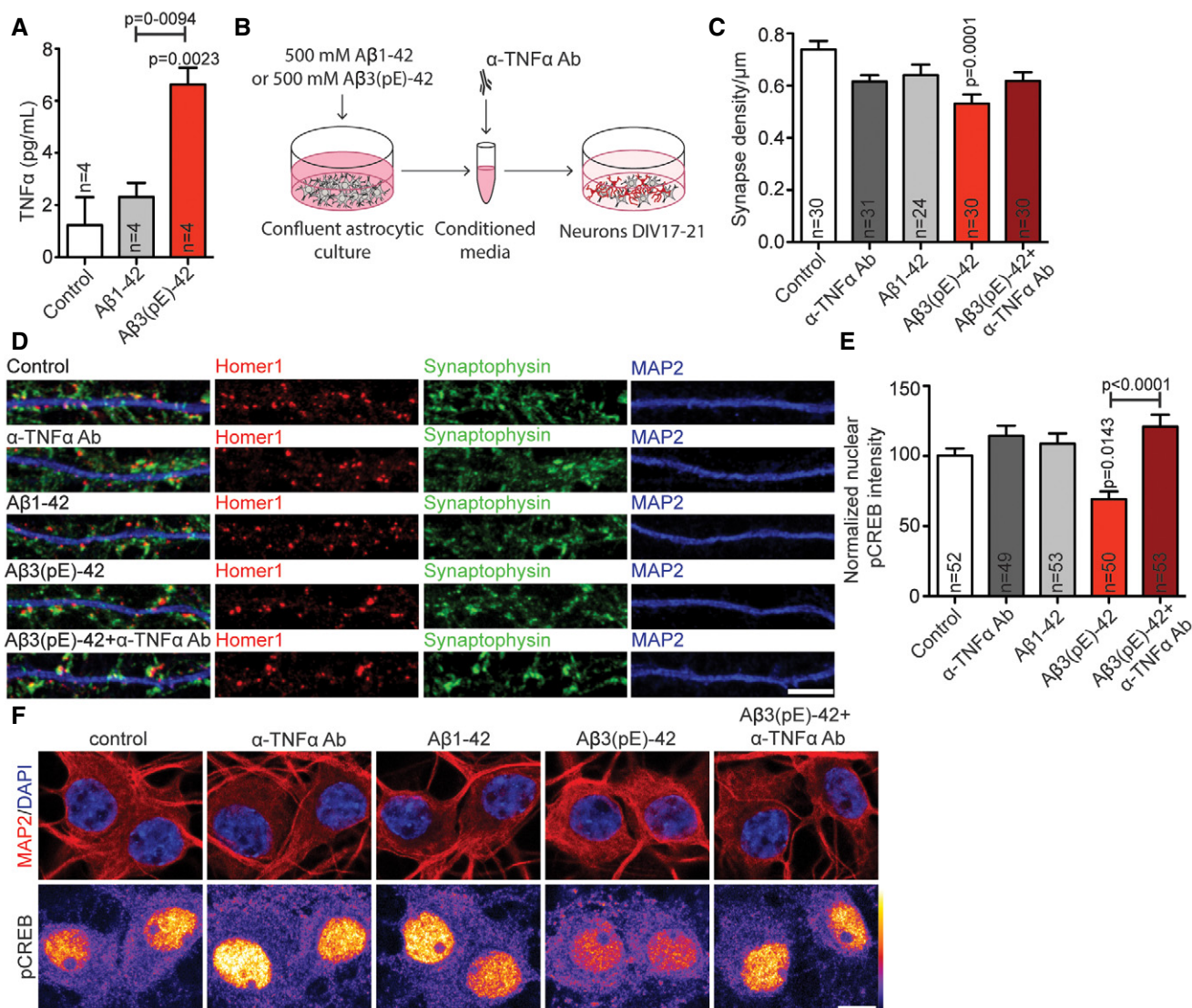


Figure 7. A β 3(pE)-42 causes astrocytic TNF α -driven synaptic dysfunction.

A Bar plot representing TNF α content in astrocytic lysate after treatment with A β 1-42 or A β 3(pE)-42 measured by ELISA. Only in case of A β 3(pE)-42, there is significant increase in TNF α . *n* corresponds to the number of flasks from 2 different experiments.

B Scheme representing stimulation with glia-conditioned media.

C, D Medium from astrocytes treated with A β 1-42 or A β 3(pE)-42 cause decrease in synaptic density only in case of A β 3(pE)-42. The depletion with anti-TNF α antibody prevents synaptic loss. *n* corresponds to the number of separate dendritic segments on different neurons analysed from at least three independent coverslips and at least two independent cell cultures. (D) Confocal images of representative dendrites stained for Homer1, Synaptophysin and MAP2. Scale bar, 5 μ m.

E The decrease in nuclear pCREB intensity occurs only in case of media from astrocytes treated with A β 3(pE)-42 and can be rescued by depletion with an anti-TNF α antibody (Ab). *n* corresponds to the number of nuclei from different neurons analysed from at least four independent coverslips and at least two independent cell cultures.

F Confocal images of DIV18 neurons stained for pCREB. Original pixel intensities from 0 to 255 are represented as a gradient lookup table. Scale bar, 10 μ m.

Data information: *P*-values versus control by one-way ANOVA. Data are represented as the mean \pm s.e.m.

Discussion

Several posttranslational modifications have been reported for A β , and heterogeneous A β species have been found in AD brain. Nonetheless, the role and abundance of numerous PTM A β have been a matter of controversy. In the present study, we focused on N-terminally modified oligomeric pyroglutamated A β that is highly

neurotoxic, efficiently nucleates A β oligomer formation and is abundant in AD [13,14,54]. The nature of the toxic role of different PTM A β species and here in particular of pyroglutamated oligomers is not clear. In consequence, it was important to learn whether propensity for oligomerisation alone, or distinct pathological signalling or a combination of both contribute to their impact on the onset of AD. In this study, we provide evidence that A β 3(pE)-42 induces

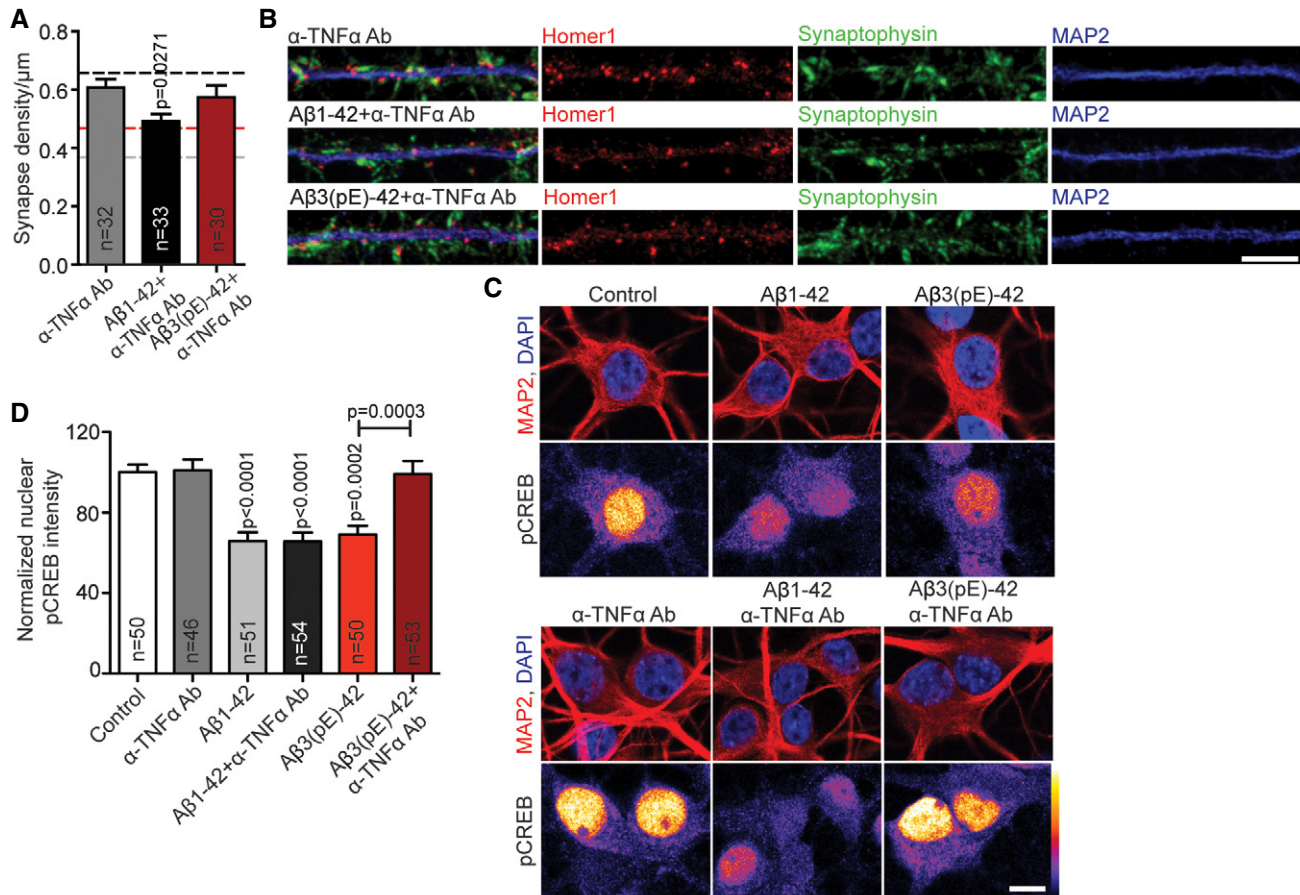


Figure 8. Co-application of anti-TNF α antibody prevents A β 3(pE)-42-caused synaptic loss and decrease in pCREB.

- A** Bar plots representing mean synapse density after treatment with anti-TNF α antibody alone or with A β 1-42 or A β 3(pE)-42 co-application. Anti-TNF α antibody fully prevents synaptic loss only in case of A β 3(pE)-42. In case of A β 1-42 application, the antibody treatment provides a partial rescue. Dashed lines indicate mean synapse density from Fig 1B: black, control; grey, A β 1-42 treatment; red, A β 3(pE)-42 treatment. *n* corresponds to the number of nuclei from different neurons analysed from at least four independent coverslips and at least two independent cell cultures.
- B** Confocal images of representative dendrites stained for Homer1, Synaptophysin and MAP2. Scale bar, 5 μm .
- C** Anti-TNF α antibody does not cause CREB shut-off and prevents A β 1-42- or A β 3(pE)-42-caused decrease in nuclear pCREB levels. Original pixel intensities from 0 to 255 are represented as a gradient lookup table. Scale bar, 10 μm .
- D** Bar plot representing mean nuclear pCREB staining intensity. *n* corresponds to the number of nuclei from different neurons analysed from at least four independent coverslips and at least two independent cell cultures.

Data information: *P*-values versus control, by one-way ANOVA. Data are presented as the mean \pm s.e.m.

synaptic dysfunction by clearly different mechanisms than A β 1-42. Application of both oligomers resulted in synapse loss, dendrite retraction, reduced mEPSC amplitude and frequency, impairment of LTP, reduced frequency of synchronised Ca²⁺ waves, CREB shut-off and nuclear import of non-phosphorylated Jacob (Appendix Fig S5). Thus, we found that A β 3(pE)-42 can induce synaptic dysfunction on its own without co-oligomerisation with A β 1-42. Many findings indicate that A β 1-42 acutely evokes synaptotoxicity by an abnormal interaction of PrP, mGlu5 and NMDAR [17,18,20,22–25,37,38]. Accordingly, we found evidence for binding of A β 1-42 to the PrP and that A β 1-42 application results in a tight association of mGlu5 and NMDAR to the PrP, thereby extending previous work and providing first evidence for an interaction in a trimeric complex (Appendix Fig S5). However, we found no evidence of A β 3(pE)-42 binding to the PrP and A β 3(pE)-42 had no effect on the assembly of

a macromolecular complex consisting of the PrP with mGlu5 and NMDAR. In addition, it did not accumulate at neuronal membranes and did not induce neuronal dysfunction via activation of extrasynaptic GluN2B-containing NMDAR. Furthermore, blocking of the PrP with an antibody that also targets the binding site for conventional A β oligomers [23] rescued only A β 1-42-dependent CREB shut-off but was ineffective in case of A β 3(pE)-42 application. Finally, in contrast to A β 1-42, A β 3(pE)-42-induced impairment of LTP could not be rescued with a dopamine D1R/D5R-agonist (Appendix Fig S5). Instead, the data suggest that synaptic dysfunction caused by A β 3(pE)-42 requires glial uptake and increased release of the proinflammatory cytokine TNF α from activated astrocytes. Supporting evidence for this hypothesis came from LTP experiments performed in transgenic mice lines where blockage of TNF α was only effective in TBA2.1 mice that produce larger

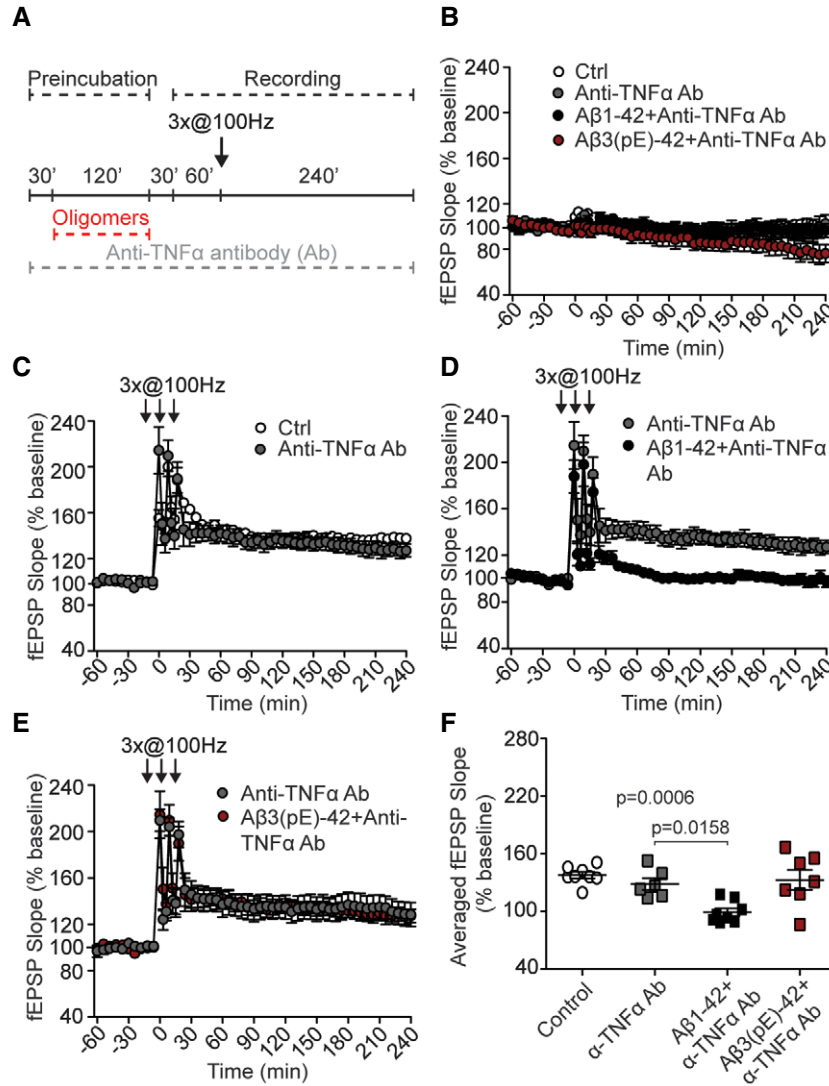


Figure 9. Anti-TNFα antibody rescues Aβ3(pE)-42- but not Aβ1-42-induced LTP impairment.

- A Scheme representing experimental design. Acute slices were preincubated with anti-TNFα antibody (Ab); then Aβ oligomers were added for 120 min. High-frequency stimulation (HFS) trains lasting 1 s at 100 Hz followed by 30-min resting period and 60-min baseline recording.
- B Anti-TNFα antibody, with or without Aβ oligomers, does not alter basal synaptic transmission (for control *n* = 6, for anti-TNFα antibody *n* = 8, for Ab1-42 co-application *n* = 8, and for Ab3(pE)-42 co-application *n* = 7).
- C Anti-TNFα antibody (*n* = 6) does not change LTP compared to control (*n* = 8).
- D, E (D) Anti-TNFα antibody does not rescue Aβ1-42- (*n* = 8) but (E) Aβ3(pE)-42-caused (*n* = 7) impairment.
- F Dot plot representing averaged fEPSP slope. *n* corresponds to the number of slices from at least three mice.

Data information: *P*-values versus control, by one-way ANOVA of averaged values measured 210–240 min posttetanisation. Data are presented as mean ± s.e.m.

amounts of Aβ3(pE)-42. Indirectly, these experiments also suggest that endogenous Aβ1-42 and Aβ3(pE)-42 oligomers have similar properties like those prepared *in vitro*.

TNFα was identified as the principle neurotoxic agent resulting from Aβ-induced proinflammatory transcriptional changes [27,44,52,55]. The cytokine contributes to impairment of synaptic plasticity [53], and it was shown that levels of TNFα correlate with the risk of development of mild cognitive impairment in AD [53]. Mounting evidence supports the hypothesis that inflammatory mediators can also affect neuronal functioning long before structural damage and cell death are observed. Indeed, several cytokines,

including IL-1β, IL-18, IFN-γ and TNFα, have been shown to suppress LTP in the hippocampus [28,53]. In addition, evidence was provided that astrocytes have a potential role in internalisation and degradation of Aβ [56,57] as well as they are a main source of ApoE whose polymorphism (ε-4 version) is the main genetic risk factor in AD [58]. It is important to note, however, that astrocytes are not the only source of proinflammatory signalling in brain. Microglia is able to bind soluble Aβ oligomers, which results in increased production of proinflammatory cytokines, including TNFα [28]. In the present study, we have used primary culture system that eases investigation but lacks microglia. The experiments with

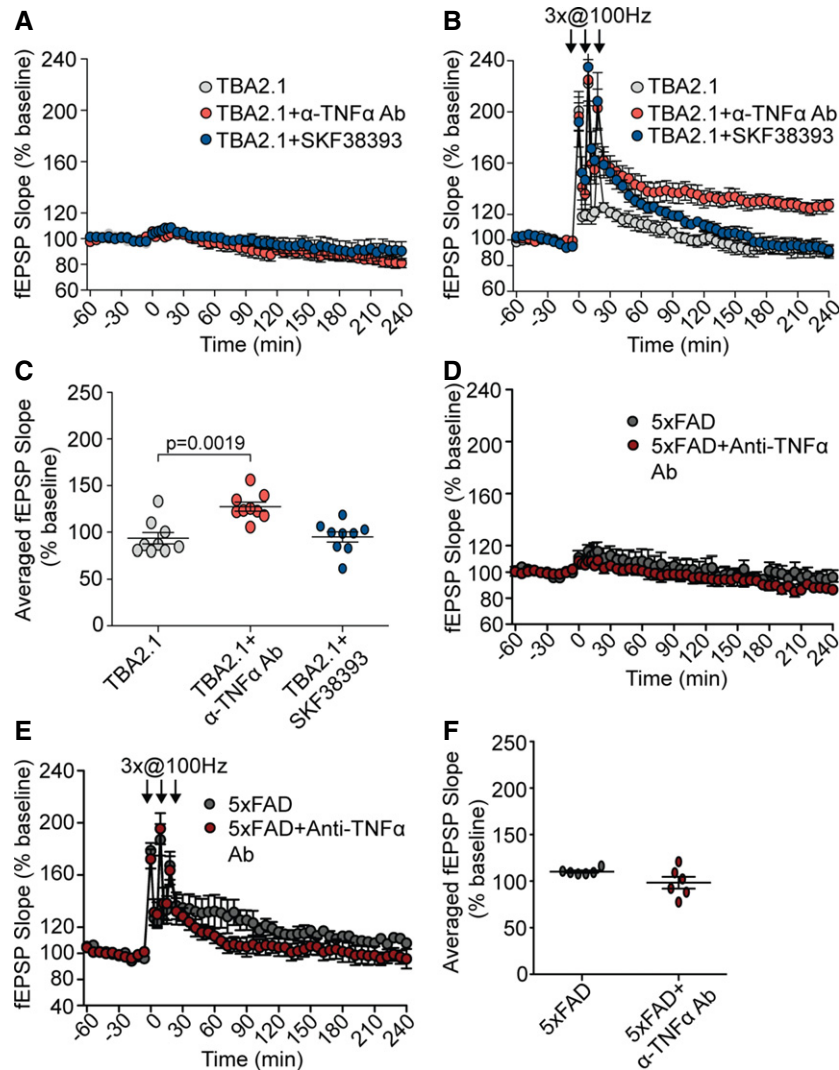


Figure 10. Anti-TNF α antibody rescues LTP impairment in TBA2.1 but not 5XFAD mice.

- A Anti-TNF α ($n = 9$) antibody and SKF38393 ($n = 7$) do not change the basal synaptic transmission in TBA2.1 mice ($n = 9$).
- B Anti-TNF α antibody ($n = 9$) but not SKF38393 ($n = 7$) rescues LTP impairment in TBA2.1 mice ($n = 9$).
- C Dot plot representing averaged fEPSP slope of values measured 210–240 min posttetanisation for TBA2.1 with and without anti-TNF α antibody ($n = 9$) or SKF38393 ($n = 7$).
- D Anti-TNF α antibody does not change the basal synaptic transmission in 5XFAD mice ($n = 6$).
- E The anti-TNF α antibody ($n = 6$) treatment does not rescue LTP impairment in 5XFAD mice ($n = 6$).
- F Dot plot representing averaged fEPSP slope of values measured 210–240 min posttetanisation for 5XFAD mice with and without anti-TNF α antibody ($n = 6$). n corresponds to the number of slices from at least five TBA2.1 mice and 4 5XFAD mice.

Data information: P -values versus control by unpaired two-tailed Student's t -test. Data are presented as mean \pm s.e.m.

organotypic slices, however, clearly showed microglia activation which was more prominent in case of A β 3(pE)-42 than the one induced by A β 1-42, a finding that has been previously reported [51]. Thus, it is highly likely that in AD brain both astrocytes and microglia contribute to the proinflammatory effects of A β 3(pE)-42 oligomers.

In summary, the present study highlights the possibility that a variety of PTM A β oligomers might not only contribute to different rates of oligomerisation, protofibril and fibril production, which results in distinct A β -deposits in AD brain at the late stage of the disease, but that they can also trigger synaptic dysfunction on their

own via different pathological signalling pathways. Collectively, the data point to a scenario where neuroinflammatory processes together with direct synaptotoxic effects are caused by soluble amyloid oligomers and contribute synergistically to the onset of AD [1–3,27–29,47]. An intriguing question is how mixed A β oligomer species will impact on the early stage of AD and trigger synaptic dysfunction and which type of oligomer will dominate in the progression of the disease in terms of abundance and pathological impact. Since signalling evoked by mixed A β species can be different, it is possible, if not likely, that there is a considerable variability in the levels of PTM A β isoforms between AD patients,

resulting in different oligomerisation rates and signalling mechanisms, and we speculate that this aspect could lead to different clinical trajectories. A nodal point in pathological signalling of both oligomers appears to be p38MAPK that is upstream of CREB shut-off and possibly also immediate synaptic dysfunction. Thus, downstream targets of synaptic signalling induced by A β 1-42 and A β 3(pE)-42 might be shared and are interesting targets for pharmacological interventions (Appendix Fig S5).

Materials and Methods

A β -oligomer production

Human A β -oligomers (Anaspec, Cat. No. AS-20276) were prepared according to previously established protocol [59]. Briefly, the lyophilised A β 1-42 was disaggregated in 1,1,1,3,3,3-hexafluoro-2-propanol (HFIP, Sigma-Aldrich, St Louis, MO, USA, Cat. No. B2517) to 0.5 mg/ml. The solution was aliquoted. After evaporating of HFIP, the peptide film was stored at -80°C . Twenty-four hours before use, the peptide film was dissolved in DMSO (1:1,000, Sigma-Aldrich, Cat. No. 276855), sonicated, diluted to 50 μM concentration in F12 medium (Gibco; Cat. No. 21765-029) and kept for oligomerisation at 4°C for 24 h. A β 3(pE)-42 oligomers (kind gift from H. Demuth) were prepared according to previously established protocol [12]. The peptide was disaggregated in HFIP, and the aliquots were stored at -80°C . HFIP was evaporated for 24 h at room temperature. The peptide was dissolved in 0.1 M NaOH, vortexed, diluted in neurobasal medium (Gibco, Cat. No. 21103049) and 0.1 M HCl to a final concentration of 5 μM . Oligomers were formed during incubation for 24 h. Since we used two different preparation protocols, for initial characterisation, part of A β 1-42 was prepared according to the A β 3(pE)-42 protocol. The oligomerisation procedure was verified by SDS-PAGE (10% Tricine gels). Membranes were probed with antibodies detecting the N-terminus of A β peptide—82E1 (1:1,000, IBL, Cat. No. 10323) and A β pE-3 (1:1,000, SySy, Cat. No. 218003), for A β 1-42 and A β 3(pE)-42, respectively. To prepare co-oligomers, 5% A β 3(pE)-42 and 95% A β 1-42 were mixed to a final 5 μM concentration and incubated for 24 h like described in [12]. For every independent experiment, the fresh preparation of oligomers was used.

Size-exclusion chromatography and ELISA assay

To further determine the distribution of different oligomer species, the oligomer solution (5 μM) was fractionated on a Superdex-75 column (GE Healthcare, Cat. No. 17-5174-01). Fractions of 1.5 ml were collected, and the amount of oligomers in each fraction was quantified by enzyme immunoassay x-42, with an antibody targeted against the C-terminus of A β peptides (IBL International, Cat. No. RE59721). A 23.56 ml Superdex column was calibrated with protein standards (aprotinin, MW 6,500; ribonuclease, MW 13,700; bovine erythrocyte carbonic anhydrase, MW 29,000; ovalbumin, MW 44,000; and conalbumin, MW 75,000; Sigma-Aldrich). Equation describing relation between elution volume and MW was obtained by plotting K_{av} ($K_{av} = (V_e - V_o)/(V_t - V_o)$; V_e , elution volume; V_o , column void volume; V_t , total column volume) versus MW. Elution volumes were determined by measuring absorbance at 280 nm.

Native PAGE

Both peptide solutions were mixed with equivolume native gel sample buffer (Bio-Rad, Cat. No. 1610738) and loaded onto native polyacrylamide gel (Mini-PROTEAN TGX, 4–20%; Bio-Rad, Cat. No. 4561096). Bands were resolved using 25 mM Tris running buffer containing 192 mM glycine followed by staining with Coomassie G250.

Dynamic light scattering measurement

Particle volume distribution based on intensity was obtained for monomer, oligomer and fibril of both peptides in 50 mM Tris buffer (pH 7.4) containing 100 mM NaCl postcentrifugation and filtration using Zetasizer Nano S DLS instrument (Malvern Instruments).

ANS spectroscopy

Fluorescence emission spectra of ANS were measured on a Hitachi F7000 spectrofluorometer. All spectra were recorded in correct spectrum mode of the instrument using excitation and emission band passes of 5 nm. 50 μM ANS was added to peptide solution (prepared in neural basal media), incubated for 2 min, and spectra were recorded between 400 and 700 nm by exciting the solution at 370 nm.

Transmission electron microscopy

Solutions were prepared as described above and stored at -20°C . Samples (5 μl) dropped on parafilm, and Formvar/carbon-coated 200-mesh copper grids (Plano, Germany) were incubated for 5 min onto the solution. After three washing steps with distilled water, the liquid was removed with wet filter paper, and the samples were negatively stained with 2% uranyl acetate for 30 s and left to dry. The samples were examined with a Zeiss 902 electron microscope operating at an excitation voltage of 80 kV equipped with a TRS 2K digital camera (A. Tröndle, Moorenweis, Germany).

Amyloid fibrils preparation and Thioflavin T assay

Amyloid peptides (A β 1-42 or A β 3(pE)-42) were diluted to 40 μM concentration and mixed with 20 μM Thioflavin T (Sigma-Aldrich, Cat. No. T3516) aqueous solution or neurobasal medium in a 1:1 ratio. Dilutions were prepared in 96-well plates (Corning). Fluorescence intensity (excitation 440 nm, emission 475–30 nm) was measured every 5 min for 7 h using a FLUOstar Omega Microplate Reader (BMG Labtechnologies, Offenburg, Germany). After successful fibril formation judged by wells containing ThT, A β fibrils diluted in neurobasal were applied to neurons for control experiments.

Primary rat hippocampal cell culture and transfection

Dissociated hippocampal neurons were prepared like described in [33]. Briefly, from Sprague Dawley rat embryos (E18) were plated on 18-mm glass coverslips coated with poly-D-lysine. For transfection, neurons were plated at a density of 60,000 and for ICC 40,000 in 12-well plate. Neurons were plated in 1 ml of DMEM supplemented with 10% FBS, 2 mM glutamine and 1% of penicillin/streptomycin.

After first day in culture, medium was changed to 1 ml of neurobasal with B27, 1% of penicillin/streptomycin and 0.8 mM glutamine. Cultures were kept at 37°C, 5% CO₂ and 95% humidity. After 5 DIV, some cultures were treated with 200 nM AraC. For Sholl analysis, neurons were transfected with GFP or RFP with Lipofectamine 2000 (Thermo Fisher Scientific, Cat. No. 11668027).

Primary rat glial culture

Glia culture was prepared from P0 rat forebrain. Following trypsinisation, cells were mechanically dissociated and plated in DMEM (Gibco, Cat. No. 41966-029) supplemented with 10% FBS, 1% penicillin/streptomycin and 0.5 mM glutamine. After 1 week when the culture reached confluency, the plate was shaken to remove microglia. For splitting, the cultures were washed with HBSS and trypsinised for 5 min at 37°C. Cells were suspended in 10 ml of supplemented DMEM and plated in 1:1 dilution in 6-well plate (for conditioned media experiments) or 12-well plates with poly-D-lysine-coated coverslips (for imaging experiments). The cells used in experiments were passaged 2–3 times. For part of the 3D reconstruction, astrocytes were transfected with myristoylated GFP with Lipofectamine 2000 (Thermo Fisher Scientific, Cat. No. 11668027).

Neuronal stimulation

A β oligomers or fibrils were added to the culture at DIV17–21 for 40 min or 3 days at 500 nM final concentrations (DMSO control diluted 1:10,000). To block binding site of PrP to A β oligomers, cells were incubated for 30 min with anti-PrP (6D11) mouse monoclonal antibody (Covance, Cat. No. SIG-39810) diluted 1:500 prior to treatment with A β oligomers. In TNF α neutralising experiments, a TNF α neutralisation antibody (1:5,000, R&D Systems, Cat. No. AF-510-NA) or 20 μ M of WP9QY (Bachem, Cat. No. N-1685) (TNFR antagonist [48]) was co-applied with A β os. To block GluN2B, 5 μ M ifenprodil (Tocris, Cat. No. 0545) was co-applied together with A β oligomers. For TNF stimulation, 1.8 nM rat TNF α (PeproTech, Cat. No. 400-14) was applied to the culture for 40 min. For inhibition of p38MAPK, 10 μ M SB203580 (Cell Signaling, Cat. No. 5633) was applied 30 min prior to A β oligomer or 1.8 nM TNF α treatment. For experiments with glia-conditioned media, astrocytic cultures were treated for 40 min with A β oligomers, cells were fixed and stained, and the medium was used for neuronal stimulation or ELISA assay. For TNF α experiments, conditioned media was incubated for 24 h with or without anti-TNF α antibody at 4°C. Afterwards, the medium was brought to 37°C and applied to neurons in a ratio of 400 μ l of neuronal media and 350 μ l of glia-conditioned media per well of 12 well plate.

TNF α ELISA

For TNF α ELISA, astrocytes were plated on T75 flask. Prior to application of A β oligomers, the supplemented DMEM was changed to serum-free DMEM. 500 nM of A β 1-42 or A β 3(pE)-42 was added to the cultures. After 13 h, the medium was collected and cells were lysed in 3 ml of hypotonic buffer (10 mM HEPES, 1.5 mM MgCl₂, 10 mM KCl) for 20 min. The lysate was briefly spun down and assayed with rat TNF α Quantikine ELISA (R&D Systems, Cat. No. RTA00) according to the manufacturer's protocol.

HEK293T transfection

Confluent HEK293T cells were transfected with calcium phosphate method with PrP-GFP or GPI-GFP (kind gift from M. Heine). One day after transfection, cells were treated with A β oligomers for 40 min, fixed and stained as described below.

Neuronal extracts preparation and immunoblotting

Dissociated, rat, hippocampal cell cultures at DIV17–19 were treated for 40 min with A β 1-42 or A β 3(pE)-42 oligomers. The coverslips were washed with ice-cold Tris-buffered saline (TBS), and the neurons were scrapped in TBS with protease inhibitor cocktail (Sigma-Aldrich, Cat. No. 000000011836170001) and phosphatase inhibitor cocktail (Sigma-Aldrich, Cat. No. 00000004906845001). The extracts were separated on 5–20% gradient gels by SDS-PAGE. For p38MAPK activation, the membranes were probed with antibodies detecting rabbit (rb) anti-phospho-p38MAPK (1:1,000, Cell Signaling, Cat. No. 9211) or rb anti-p38MAPK (1:1,000, Cell Signaling, Cat. No. 9212). All membranes were subsequently probed with rb anti-histone 3 (1:1,000, New England Biolabs, Cat. No. 4499) antibody as a loading control. To test for presence of microglia, the membranes were cut and probed with antibodies detecting guinea pig (gp) anti-Iba-1 (1:1,000, SySy, Cat. No. 234 004), rb anti-GFAP (1:1,000, Sigma-Aldrich, Cat. No. G-9269) or mouse (ms) anti-NeuN (1:1,000, Millipore, Cat. No. MAB 377) with organotypic slices extract prepared in similar way as neuronal extract as positive control.

Immunocytochemistry

Following stimulation, cells were fixed in 4% paraformaldehyde (PFA) for 10 min at room temperature. After washing in PBS, cells were blocked for 1 h at room temperature in blocking buffer (2% glycine, 2% BSA, 0.2% gelatine and 50 mM NH₄Cl). The primary antibodies were applied rb anti-pJacob-Ser180 [33] (1:500), rb anti-Jacob [60] (1:300), rb anti-pCREB Ser133 (1:500, Cell Signalling, Cat. No. 9198), rb anti-CREB (1:500, Cell Signalling, Cat. No. 4820), ms anti-A β 1-42, clone 82E1 (1:1,000, IBL, Cat. No. 10323), rb anti-A β 3(pE)-42 (1:1,000, SySy, Cat. No. 218 003), gp anti-Synaptophysin (1:500, SySy, Cat. No. 101 004), ms anti-Homer1 (1:500, SySy, Cat. No. 160 001), gp anti-Iba-1 (1:500, SySy, Cat. No. 234 004), rb anti-GFAP (1:1,000, Sigma-Aldrich, Cat. No. G-9269) and were diluted in blocking buffer and incubated overnight at 4°C. Following incubation with primary antibody, coverslips were washed in PBS and incubated for 1 h at room temperature with secondary antibodies diluted 1:1,000 in blocking buffer conjugated with Alexa Fluor (AF); donkey anti-rabbit AF568 (1:750, Invitrogen, Cat. No. A10042), goat anti-mouse AF647 (1:750, Invitrogen, Cat. No. A-21235). After washing for 1 h, cells were incubated with pre-labelled (AF488) anti-MAP2 antibody (1:1,000, Millipore, Cat. No. AB2290A4) or phalloidin conjugated with AF488 (1:1,000, Thermo Fisher Scientific, Cat. No. A12379). The coverslips were extensively washed and incubated with 1 μ g/ml DAPI (Sigma-Aldrich, Cat. No. D9542) in PBS. Coverslips were mounted in Mowiol (Polysciences Inc., Cat. No. 17951) and kept at 4°C.

Confocal laser scan microscopy and quantitative ICC

Images were acquired using Leica TCS SP5. To quantify changes of pCREB, CREB, pJacob and Jacob in the nucleus cell somas were scanned sequentially with detection of AF568, AF488 (for MAP2) and DAPI. The optical sections were acquired along Z-axis with 0.42 μ m Z resolution. Fiji program [61] was used for intensity quantification. Two nuclear sections were overlaid, and staining intensity (in arbitrary units of pixel intensity) was measured within regions of interest (ROI) defined by DAPI staining. The images showing localisation of A β oligomers in glial or neuronal culture were also acquired with confocal microscope. The cells were selected on the basis of phalloidin (glia culture) or MAP2 staining and scanned sequentially with detection of AF568 (A β 3(pE)-42) or AF647 (A β 1-42). The scan parameters were set based on control cells stained without primary antibody. For representative images, linear contrast enhancement was applied. Final figures were prepared with Adobe Illustrator software. For 3D reconstruction of astrocytes, images were acquired with 0.250 μ m Z resolution and processed with Imaris (Bitplane) software. For visualisation purpose, the phalloidin or myristoylated GFP (mGFP) channel was used to create a semi-transparent surface.

Synapse quantification and Sholl analysis

On DIV21 500 nM A β oligomers were applied for 3 days. To quantify synapse number, images of secondary dendrites (MAP2), Synaptophysin and Homer1 were acquired with fluorescent microscope (Zeiss Imager A2, 63 \times objective). The images were processed in Fiji software, applying 0.1% histogram normalisation (synaptic staining channel, all analysed pictures). After creating composite image for Homer1 and Synaptophysin, colocalising signals were counted on the dendritic branches of ca. 30 μ m length. To ensure better image quality, representative images were acquired with Leica TCS SP5 microscope. For Sholl analysis, images of GFP- or RFP-transfected neurons were acquired with fluorescence microscope (Zeiss Imager A2, 10 \times objective). The concentric circles (radius step 10 μ m) were drawn with Concentric Circles Fiji plug-in. The crossings of dendrites with each circle were counted manually by a researcher blind to the experimental conditions.

Whole-cell voltage-clamp recording of mEPSCs

Miniature excitatory postsynaptic currents (mEPSCs) of hippocampal primary neurons (DIV16–18) were recorded under whole-cell voltage-clamp conditions using 3–5 M Ω pipettes filled with an intracellular solution containing (in mM): KCl 135, EGTA 1, HEPES 10, Mg²⁺-ATP 4, Na-GTP 1, pH 7.4 with KOH (290 mOsm). 0.5 μ M tetrodotoxin (TTX, Tocris, Cat. No. 1078) and 5 μ M bicuculline were routinely added to the extracellular solution containing (in mM): NaCl 140, KCl 5, CaCl₂ 2, MgCl₂ 0.8, HEPES 10, glucose 10, pH 7.4 with NaOH (300 mOsm), to block spontaneous action potential generation and GABA_A receptors. Neurons plated on coverslips were transferred to a RC26 GLP recording chamber (Warner Instruments, USA) mounted on a Leica TCS SP2 microscope equipped with 40 \times water dipping objective and were perfused with extracellular solution at a rate of 1 ml/min. The temperature in the recording chamber (25°C) was controlled by a TC344B dual temperature

controller (Warner Instruments). The perfusion of external solution was switched off to add DMSO or A β oligomers to the chamber. The volume of the external solution inside the chamber was kept at 1 ml, and 10 μ l DMSO, 10 μ l A β 1-42 and 100 μ l A β 3(pE)-42 were added to achieve the final concentrations of 500 nM amyloid A β 1-42 and A β 3(pE)-42. mEPSCs were recorded between 10 and 45 min after the addition of DMSO or the peptides mentioned. Axopatch 200B (Molecular Devices, USA) amplifier controlled with Clampex 10 software (Molecular Devices) was used for recording the mEPSC current traces. Membrane potential was held at –60 mV, and current traces were filtered at 2 kHz low-pass basal filter and digitised at 10 kHz with Digidata 1440A (Molecular Devices, USA). Continuous recording of current traces were followed by offline analysis by using Minianalysis 6 software, and Prism 5 was used for statistical analysis. Only whole-cell voltage-clamp recordings from cells with a membrane resistance of 150–350 M Ω and a holding current of < 200 pA were included in the analysis.

Hippocampal organotypic slices and IHC

Hippocampi were dissected from P9 C57/B6J mice and cut into 350- μ m sections. Sections were transferred onto the membranes (Millipore) (3–4 per membrane) and cultured in OHSC medium (50% minimal essential medium (Gibco, Cat. No. 21090-022), 25% heat-inactivated horse serum (Gibco, Cat. No. 26050-088), 25 mM glucose, 2 mM glutamine, 25 mM HEPES, B27 and 1% of penicillin/streptomycin) in 37°C, 5% CO₂ and 95% humidity. After 2 days, the slices were cultured for 12 days at 35°C, 5% CO₂ and 95% humidity, with regular medium change every 3 day. Before stimulation, viability of slices was checked by means of propidium iodide uptake. A β oligomers were added directly to the medium and kept for 3 days. Then, slices were fixed for 1 h at room temperature in 4% PFA. Following fixation, slices were washed with PBS, removed from the membranes, snap-frozen on metal block three times and transferred to 48-well plate. After blocking with 20% BSA for 1.5 h at room temperature, slices were incubated with primary antibody diluted in 5% BSA gp anti-Iba-1 (1:300, SySy, Cat. No. 234 004), rb anti-GFAP (1:300, Sigma-Aldrich, Cat. No. G-9269) at 4°C. After washing with PBS, slices were incubated for 3.5 h at room temperature with secondary antibodies conjugated with Alexa Fluor diluted 1:400: donkey anti-rabbit AF568 (Invitrogen, Cat. No. A10042), goat anti-mouse AF647 (Invitrogen, Cat. No. A-21235). After washing, slices were incubated for 10 min in 1 μ g/ml DAPI (Sigma-Aldrich, Cat. No. D9542) in PBS. Sections were mounted Mowiol (Polysciences Inc., Cat. No. 17951), and images were acquired with Leica TCS SP5 20 \times water objective. Images of five focal planes were overlaid. For Iba-1-positive cells, quantification cells were counted using Imaris software on whole slice surface. For GFAP, the fluorescence intensity was measured within ROI of the same size in CA1 (selected based on DAPI) region using Fiji software.

Calcium imaging

Hippocampal neurons were treated with 500 nM A β oligomers for 3 days with or without 5 μ M ifenprodil (Tocris). 10 min prior to imaging neurons were incubated with 1 μ M Fluo-4 AM (Thermo Fisher Scientific, Cat. No. F14201). For imaging, coverslips were transferred to imaging chamber. Images of one plane were acquired

with Leica TCS SP5 63 \times objective at 37°C for 10 min at 1 Hz frequency (excitation 488 Argon laser) and saved as image stacks for further offline analysis. For each stack, 4–6 ROIs surrounding perisomatic region of neurons were manually selected for calculation of the mean fluorescence over time. After removal of low-frequency DC component (time constant 10 s), resulting temporal profiles were used for threshold-based detection of calcium spikes (\pm 4 standard deviations computed separately for each cell). Calcium spikes were considered as synchronised if they occurred within the sliding detection window (width 1 s) in two or more individual cells. Signal processing and detection of spikes were carried out using Spike2 software (Cambridge Electronic Design, Cambridge, UK).

Bioluminescence resonance energy transfer

HEK-293T cells were co-transfected with 0.4 μ g of cDNA for GluN11a-RLuc (BRET donor), 0.4 μ g of cDNA for GluN2B-myc and with increasing amounts 0.1–1.2 μ g of cDNA for mGlu5-YFP (BRET acceptor). A subset of cells was co-transfected with 0.4 μ g of PrP. Cells were treated with 500 nM A β 1-42 or A β 3(pE)-42 for 4 h and compared to untreated control groups. To quantify GluN11a-YFP expression, cells (20 μ g protein) were kept in 96-well plates (black plates with a transparent bottom), and fluorescence was read in the Fluo Star Optima Fluorimeter using a 10 nm bandwidth excitation filter at 400 nm reading. Protein fluorescence expression was determined as fluorescence of the sample minus the fluorescence of cells expressing the BRET donor alone. For BRET measurements, the equivalent of 20 μ g of cell suspension was distributed in 96-well plates (white plates) and 5 μ M coelenterazine H (Molecular Probes, Cat. No. C6780) was added. After 1 min, the readings were collected using a Mithras LB 940 (Berthold Technologies, Germany) that allows the integration of the signals detected in the short-wavelength filter at 485 nm and the long-wavelength filter at 530 nm. To quantify mGlu5-RLuc expression, luminescence readings were also performed after 10 min of adding 5 μ M coelenterazine H. The averages come from at least three independent experiments.

TBA2.1 and 5XFAD animals

The 5XFAD (+/–) animals [62] were kind gift from Prof. Dr. A. Dityatev. The TBA2.1 (tg/tg) mice were kind gift from ProBiodrug. These mice overexpress the A β 3(pE)-42 peptide driven by Thy-1 promoter. The upstream sequence coding for pre/pro-peptide of murine thyrotropin-releasing hormone leads to cleavage within the trans-Golgi and vesicular secretion of A β 3(pE)-42 [51]. Both lines had C57BL/6 background.

Acute hippocampal slices, measurement of baseline activity and LTP

Hippocampal slices from C57/B6J mice (12–16 weeks old, male), 5XFAD (+/–, 44–47 weeks old, female, n = 4) or TBA2.1 (tg/tg, 12–14 weeks old, male, n = 6) were prepared according to previously described protocol [41]. Slices from C57/B6J mice were placed in pre-chamber for 2 h with 500 nM A β oligomers. For rescue experiment, SKF38393 (5 μ M, Tocris, Cat. No. 0922) was co-applied with oligomers or slices were incubated for 30 min with 0.2 μ g/ml

anti-TNF α antibody prior to incubation with oligomers. The anti-TNF α antibody was present throughout the complete experiment. Next, slices were left to recover for at least 30 min in the recording chamber. Field excitatory postsynaptic potentials (fEPSPs) were measured in stratum radiatum after stimulation of CA1 Schaffer-collateral fibres with ACSF glass capillary microelectrodes (3–5 M Ω). fEPSPs were amplified by Extracellular Amplifier (EXT-02B, npi, Germany) and digitised at a sample frequency of 5 kHz by Digi-data 1201 plus AD/Da converter (CED, UK). The strength of stimuli was adjusted to 40–50% of the maximum fEPSP slope values. Single stimuli were applied at 0.0333 Hz and averaged every 5 min. Stable baseline recordings were followed by tetanisation with 3 \times 1 s stimulus trains at 100 Hz with a 10-min inter-train interval and double-pulse width (0.2 ms).

Statistics

Statistical analyses were carried out with GraphPad Prism software. Data are represented as mean \pm s.e.m. One-way ANOVA followed by Tukey's multiple comparison test or two-tailed Student's t -test was used for comparison of groups. For Sholl analysis, two-way ANOVA was used to compare variances; for comparison of single points, Student's t -test was used. For LTP experiments, averages from 210 to 240 min posttetanisation were compared by one-way ANOVA followed by Bonferroni's multiple comparison test. For Ca²⁺ imaging, one-way ANOVA followed by Duncan's multiple comparison test was performed separately for groups with and without ifenprodil. For quantification of immunoblots, a Mann–Whitney U -test was used.

Expanded View for this article is available online.

Acknowledgements

The authors gratefully acknowledge the professional technical assistance of C. Borutzki, S. Hochmuth and M. Marunde. We would like to thank O. Kobler and T. Stöter for support in the image analysis; D. Ramsbeck for synthesis of A β ; M. Wermann and D. Schlenzig for help with SEC and the ThT assay; and M. Heine for providing plasmids. Supported by grants from the Bundesministerium für Bildung und Forschung "Energi" FKZ: 01GQ1421B, Deutsche Forschungsgemeinschaft (DFG Kr1879/5-1, 6-1; SFB779 TPB8), The EU Joint Programme—Neurodegenerative Disease Research (JPNDR) project STAD, WGL Pakt f. Forschung, People Programme (Marie Curie Actions) of the European Union's Seventh Framework Programme FP7/2007-2013/under REA grant agreement no. [289581], H2020 Priority Excellent Science, Marie Skłodowska-Curie Actions (MSCA) MC-ITN NPlast, and Pakt für Forschung by Leibniz-Association.

Author contributions

KMG and MRK designed the study and wrote the paper. KMG performed experiments and data analysis excluding: LTP experiments performed by PY; BRET experiments by GB; mEPSC recordings by GS; native PAGE, DLS, ANS performed by RR; TEM performed by MS; and Ca²⁺ traces analysis performed by AB. JB contributed to establishment of readouts, preparation and characterisation of A β oligomers, organotypic slices culture and staining protocol. H-UD and SS provided A β 1-42 and A β 3(pE)-42. H-UD and MRK supervised the project.

Conflict of interest

The authors declare that they have no conflict of interest.

References

- Selkoe DJ, Hardy J (2016) The amyloid hypothesis of Alzheimer's disease at 25 years. *EMBO Mol Med* 8: 595–608
- Viola KL, Klein WL (2015) Amyloid beta oligomers in Alzheimer's disease pathogenesis, treatment, and diagnosis. *Acta Neuropathol* 129: 183–206
- Jawhar S, Wirths O, Bayer TA (2011) Pyroglutamate amyloid-beta (A β): a hatchet man in Alzheimer disease. *J Biol Chem* 286: 38825–38832
- Kummer MP, Heneka MT (2014) Truncated and modified amyloid-beta species. *Alzheimers Res Ther* 6: 28
- Saido TC, Yamao-Harigaya W, Iwatsubo T, Kawashima S (1996) Amino- and carboxyl-terminal heterogeneity of beta-amyloid peptides deposited in human brain. *Neurosci Lett* 215: 173–176
- Bayer TA, Wirths O (2014) Focusing the amyloid cascade hypothesis on N-truncated A β peptides as drug targets against Alzheimer's disease. *Acta Neuropathol* 127: 787–801
- Hosoda R, Saido TC, Otvos L Jr, Arai T, Mann DM, Lee VM, Trojanowski JQ, Iwatsubo T (1998) Quantification of modified amyloid beta peptides in Alzheimer disease and down syndrome brains. *J Neuropathol Exp Neurol* 57: 1089–1095
- Harigaya Y, Saido TC, Eckman CB, Prada CM, Shoji M, Younkin SG (2000) Amyloid beta protein starting pyroglutamate at position 3 is a major component of the amyloid deposits in the Alzheimer's disease brain. *Biochem Biophys Res Commun* 276: 422–427
- Perez-Garmendia R, Gevorkian G (2013) Pyroglutamate-modified amyloid beta peptides: emerging targets for Alzheimer's disease immunotherapy. *Curr Neuropharmacol* 11: 491–498
- Saido TC, Iwatsubo T, Mann DM, Shimada H, Ihara Y, Kawashima S (1995) Dominant and differential deposition of distinct beta-amyloid peptide species, A β N3(pE), in senile plaques. *Neuron* 14: 457–466
- Mandler M, Rockenstein E, Ubhi K, Hansen L, Adame A, Michael S, Galasko D, Santic R, Mattner F, Masliah E (2012) Detection of perisynaptic amyloid-beta pyroglutamate aggregates in early stages of Alzheimer's disease and in A β PP transgenic mice using a novel monoclonal antibody. *J Alzheimers Dis* 28: 783–794
- Nussbaum JM, Schilling S, Cynis H, Silva A, Swanson E, Wangsanut T, Tayler K, Wiltgen B, Hatami A, Ronicke R et al (2012) Prion-like behaviour and tau-dependent cytotoxicity of pyroglutamylated amyloid-beta. *Nature* 485: 651–655
- Schlenzig D, Manhart S, Cinar Y, Kleinschmidt M, Hause G, Willbold D, Funke SA, Schilling S, Demuth HU (2009) Pyroglutamate formation influences solubility and amyloidogenicity of amyloid peptides. *Biochemistry* 48: 7072–7078
- Russo C, Violani E, Salis S, Venezia V, Dolcini V, Damonte G, Benatti U, D'Arrigo C, Patrone E, Carlo P et al (2002) Pyroglutamate-modified amyloid beta-peptides–A β N3(pE)–strongly affect cultured neuron and astrocyte survival. *J Neurochem* 82: 1480–1489
- Schilling S, Lauber T, Schaupp M, Manhart S, Scheel E, Bohm G, Demuth HU (2006) On the seeding and oligomerization of pGlu-amyloid peptides (*in vitro*). *Biochemistry* 45: 12393–12399
- Dewachter I, Filipkowski RK, Priller C, Ris L, Neyton J, Croes S, Terwel D, Gysemans M, Devijver H, Borghgraef P et al (2009) Deregulation of NMDA-receptor function and down-stream signaling in APP[V717] transgenic mice. *Neurobiol Aging* 30: 241–256
- Kessels HW, Nabavi S, Malinow R (2013) Metabotropic NMDA receptor function is required for beta-amyloid-induced synaptic depression. *Proc Natl Acad Sci USA* 110: 4033–4038
- Malinow R (2012) New developments on the role of NMDA receptors in Alzheimer's disease. *Curr Opin Neurobiol* 22: 559–563
- Shankar GM, Bloodgood BL, Townsend M, Walsh DM, Selkoe DJ, Sabatini BL (2007) Natural oligomers of the Alzheimer amyloid-beta protein induce reversible synapse loss by modulating an NMDA-type glutamate receptor-dependent signaling pathway. *J Neurosci* 27: 2866–2875
- Renner M, Lacor PN, Velasco PT, Xu J, Contractor A, Klein WL, Triller A (2010) Deleterious effects of amyloid beta oligomers acting as an extracellular scaffold for mGluR5. *Neuron* 66: 739–754
- Um JW, Kaufman AC, Kostylev M, Heiss JK, Stagi M, Takahashi H, Kerrisk ME, Vortmeyer A, Wisniewski T, Koleske AJ et al (2013) Metabotropic glutamate receptor 5 is a coreceptor for Alzheimer A β oligomer bound to cellular prion protein. *Neuron* 79: 887–902
- Wang Q, Walsh DM, Rowan MJ, Selkoe DJ, Anwyl R (2004) Block of long-term potentiation by naturally secreted and synthetic amyloid beta-peptide in hippocampal slices is mediated via activation of the kinases c-Jun N-terminal kinase, cyclin-dependent kinase 5, and p38 mitogen-activated protein kinase as well as metabotropic glutamate receptor type 5. *J Neurosci* 24: 3370–3378
- Larson M, Sherman MA, Amar F, Nuvolone M, Schneider JA, Bennett DA, Aguzzi A, Lesne SE (2012) The complex PrP(c)-Fyn couples human oligomeric A β with pathological tau changes in Alzheimer's disease. *J Neurosci* 32: 16857–16871
- Lauren J, Gimbel DA, Nygaard HB, Gilbert JW, Strittmatter SM (2009) Cellular prion protein mediates impairment of synaptic plasticity by amyloid-beta oligomers. *Nature* 457: 1128–1132
- Um JW, Strittmatter SM (2013) Amyloid-beta induced signaling by cellular prion protein and Fyn kinase in Alzheimer disease. *Prion* 7: 37–41
- Um JW, Nygaard HB, Heiss JK, Kostylev MA, Stagi M, Vortmeyer A, Wisniewski T, Gunther EC, Strittmatter SM (2012) Alzheimer amyloid-beta oligomer bound to postsynaptic prion protein activates Fyn to impair neurons. *Nat Neurosci* 15: 1227–1235
- He P, Zhong Z, Lindholm K, Berning L, Lee W, Lemere C, Staufenbiel M, Li R, Shen Y (2007) Deletion of tumor necrosis factor death receptor inhibits amyloid beta generation and prevents learning and memory deficits in Alzheimer's mice. *J Cell Biol* 178: 829–841
- Heneka MT, Carson MJ, Khoury JE, Landreth GE, Brosseron F, Feinstein DL, Jacobs AH, Wyss-Coray T, Vitorica J, Ransohoff RM et al (2015) Neuroinflammation in Alzheimer's disease. *Lancet Neurol* 14: 388–405
- Heppner FL, Ransohoff RM, Becher B (2015) Immune attack: the role of inflammation in Alzheimer disease. *Nat Rev Neurosci* 16: 358–372
- Hardingham GE, Bading H (2010) Synaptic versus extrasynaptic NMDA receptor signalling: implications for neurodegenerative disorders. *Nat Rev Neurosci* 11: 682–696
- Li S, Jin M, Koeglsperger T, Shepardson NE, Shankar GM, Selkoe DJ (2011) Soluble A β oligomers inhibit long-term potentiation through a mechanism involving excessive activation of extrasynaptic NR2B-containing NMDA receptors. *J Neurosci* 31: 6627–6638
- España J, Valero J, Minano-Molina AJ, Masgrau R, Martin E, Guardia-Laguarta C, Lleó A, Gimenez-Llort L, Rodriguez-Alvarez J, Saura CA (2010) Beta-Amyloid disrupts activity-dependent gene transcription required for memory through the CREB coactivator CRTCL1. *J Neurosci* 30: 9402–9410
- Karpova A, Mikhaylova M, Bera S, Bar J, Reddy PP, Behnisch T, Rankovic V, Spilker C, Bethge P, Sahin J et al (2013) Encoding and transducing the synaptic or extrasynaptic origin of NMDA receptor signals to the nucleus. *Cell* 152: 1119–1133
- Gomes GM, Dalmolin GD, Bar J, Karpova A, Mello CF, Kreutz MR, Rubin MA (2014) Inhibition of the polyamine system counteracts beta-amyloid

- peptide-induced memory impairment in mice: involvement of extrasynaptic NMDA receptors. *PLoS One* 9: e99184
35. Rönicke R, Mikhaylova M, Rönicke S, Meinhardt J, Schroder UH, Fandrich M, Reiser G, Kreutz MR, Reymann KG (2011) Early neuronal dysfunction by amyloid beta oligomers depends on activation of NR2B-containing NMDA receptors. *Neurobiol Aging* 32: 2219–2228
 36. Dieterich DC, Karpova A, Mikhaylova M, Zdobnova I, König I, Landwehr M, Kreutz M, Smalla KH, Richter K, Landgraf P et al (2008) Caldendrin-jacob: a protein liaison that couples NMDA receptor signalling to the nucleus. *PLoS Biol* 6: e34
 37. Hu NW, Klyubin I, Anwyl R, Rowan MJ (2009) GluN2B subunit-containing NMDA receptor antagonists prevent Abeta-mediated synaptic plasticity disruption *in vivo*. *Proc Natl Acad Sci USA* 106: 20504–20509
 38. Rush T, Buisson A (2014) Reciprocal disruption of neuronal signaling and Abeta production mediated by extrasynaptic NMDA receptors: a downward spiral. *Cell Tissue Res* 356: 279–286
 39. Jurgensen S, Antonio LL, Mussi GE, Brito-Moreira J, Bomfim TR, De Felice FG, Garrido-Sanabria ER, Cavalheiro EA, Ferreira ST (2011) Activation of D1/D5 dopamine receptors protects neurons from synapse dysfunction induced by amyloid-beta oligomers. *J Biol Chem* 286: 3270–3276
 40. Walsh DM, Klyubin I, Fadeeva JV, Rowan MJ, Selkoe DJ (2002) Amyloid-beta oligomers: their production, toxicity and therapeutic inhibition. *Biochem Soc Trans* 30: 552–557
 41. Yuan Xiang P, Janc O, Grochowska KM, Kreutz MR, Reymann KG (2016) Dopamine agonists rescue Abeta-induced LTP impairment by Src-family tyrosine kinases. *Neurobiol Aging* 40: 98–102
 42. Dohler F, Sepulveda-Falla D, Krasemann S, Altmeyen H, Schlüter H, Hildebrand D, Zerr I, Matschke J, Glatzel M (2014) High molecular mass assemblies of amyloid- β oligomers bind prion protein in patients with Alzheimer's disease. *Brain* 3: 873–886
 43. Perroy J, Raynaud F, Homburger V, Rousset MC, Telley L, Bockaert J, Fagni L (2008) Direct interaction enables cross-talk between ionotropic and group I metabotropic glutamate receptors. *J Biol Chem* 283: 6799–6805
 44. Floden AM, Li S, Combs CK (2005) Beta-amyloid-stimulated microglia induce neuron death via synergistic stimulation of tumor necrosis factor alpha and NMDA receptors. *J Neurosci* 25: 2566–2575
 45. McCoy MK, Tansey MG (2008) TNF signaling inhibition in the CNS: implications for normal brain function and neurodegenerative disease. *J Neuroinflammation* 5: 45–53
 46. Stellwagen D, Malenka RC (2006) Synaptic scaling mediated by glial TNF-alpha. *Nature* 440: 1054–1059
 47. White JA, Manelli AM, Holmberg KH, Van Eldik LJ, Ladu MJ (2005) Differential effects of oligomeric and fibrillar amyloid-beta 1-42 on astrocyte-mediated inflammation. *Neurobiol Dis* 18: 459–465
 48. Takasaki W, Kajino Y, Kajino K, Murali R, Greene MI (1997) Structure-based design and characterization of exocyclic peptidomimetics that inhibit TNF alpha binding to its receptor. *Nat Biotechnol* 12: 1266–1270
 49. Xu H, Czerwinski P, Förstermann U, Li H (2015) Downregulation of BDNF expression by PKC and by TNF- α in human endothelial cells. *Pharmacology* 2: 1–10
 50. Kimura R, Ohno M (2009) Impairments in remote memory stabilization precede hippocampal synaptic and cognitive failures in 5XFAD Alzheimer mouse model. *Neurobiol Dis* 33: 229–235
 51. Alexandru A, Jagla W, Graubner S, Becker A, Bauscher C, Kohlmann S, Sedlmeier R, Raber KA, Cynis H, Rönicke R et al (2011) Selective hippocampal neurodegeneration in transgenic mice expressing small amounts of truncated Abeta is induced by pyroglutamate-Abeta formation. *J Neurosci* 31: 12790–12801
 52. Chen X, Lin R, Chang L, Xu S, Wei X, Zhang J, Wang C, Anwyl R, Wang Q (2013) Enhancement of long-term depression by soluble amyloid beta protein in rat hippocampus is mediated by metabotropic glutamate receptor and involves activation of p38MAPK, STEP and caspase-3. *Neuroscience* 253: 435–443
 53. Wang Q, Wu J, Rowan MJ, Anwyl R (2005) Beta-amyloid inhibition of long-term potentiation is mediated via tumor necrosis factor. *Eur J Neurosci* 22: 2827–2832
 54. Schlenzig D, Rönicke R, Cynis H, Ludwig HH, Scheel E, Reymann K, Saido T, Hause G, Schilling S, Demuth HU (2012) N-Terminal pyroglutamate formation of Abeta38 and Abeta40 enforces oligomer formation and potency to disrupt hippocampal long-term potentiation. *J Neurochem* 121: 774–784
 55. Bhaskar K, Maphis N, Xu G, Varvel NH, Kokiko-Cochran ON, Weick JP, Staugaitis SM, Cardona A, Ransohoff KH, Lamb BT (2014) Microglial derived tumor necrosis factor- α drives Alzheimer's disease-related neuronal cell cycle events. *Neurobiol Dis* 62: 273–285
 56. Nielsen HM, Mulder SD, Belien JA, Musters RJ, Eikelenboom P, Veerhuis R (2010) Astrocytic A beta 1-42 uptake is determined by A beta-aggregation state and the presence of amyloid-associated proteins. *Glia* 58: 1235–1246
 57. Pihlaja R, Koistinaho J, Malm T, Sikkila H, Vainio S, Koistinaho M (2008) Transplanted astrocytes internalize deposited beta-amyloid peptides in a transgenic mouse model of Alzheimer's disease. *Glia* 56: 154–163
 58. Liu CC, Kanekiyo T, Xu H, Bu G (2013) Apolipoprotein E and Alzheimer disease: risk, mechanisms and therapy. *Nat Rev Neurol* 9: 106–118
 59. Klein WL (2002) Abeta toxicity in Alzheimer's disease: globular oligomers (ADDLs) as new vaccine and drug targets. *Neurochem Int* 41: 345–352
 60. Spilker C, Nullmeier S, Grochowska KM, Schumacher A, Butnaru I, Macharadze T, Gomes GM, Yuanxiang P, Bayraktar G, Rodenstein C et al (2016) A Jacob/Nsmf gene knockout results in hippocampal dysplasia and impaired BDNF signaling in dendritogenesis. *PLoS Genet* 12: e1005907
 61. Schindelin J, Arganda-Carreras I, Frise E, Kaynig V, Longair M, Pietzsch T, Preibisch S, Rueden C, Saalfeld S, Schmid B et al (2012) Fiji: an open-source platform for biological-image analysis. *Nat Methods* 9: 676–682
 62. Oakley H, Cole SL, Logan S, Maus E, Shao P, Craft J, Guillozet-Bongaarts A, Ohno M, Disterhoft J, Van Eldik L et al (2006) Intraneuronal β -amyloid aggregates, neurodegeneration, and neuron loss in transgenic mice with five familial Alzheimer's disease mutations: potential factors in amyloid plaque formation. *Neurobiol Dis* 26: 10129–10140